

Chapter 33. PHYSICAL AND BIOGEOCHEMICAL CHARACTERISTICS OF THE BLACK SEA (28,S)

TEMEL OGUZ, SULEYMAN TUGRUL, A. ERKAN KIDEYS, VEDAT EDIGER AND NILGUN KUBILAY

*Middle East Technical University, Institute of Marine Sciences,
Erdemli, Turkey*

Contents

1. Introduction
 2. Physical characteristics
 3. Circulation characteristics
 4. Major features of the vertical biogeochemical structure
 5. Paleoceanographic characteristics
 6. Changes in the ecosystem characteristics since 1970s
 7. Interdisciplinary modeling studies
 8. Conclusions
- Bibliography

1. Introduction

The Black Sea, located approximately between latitudes of 41° to 46°N and longitudes of 28° to 41.5°E, is an elongated and nearly-enclosed basin connected with the Bosphorus Strait to the Mediterranean Sea. It has experienced one of the worst environmental degradations of the world oceans during the last three decades. The environmental crisis and subsequent dramatic changes in the ecosystem and its resources were a direct consequence of anthropogenic pollution due to an enormous increase in nutrients and pollutant load from rivers discharging into the northwestern region of the sea, uncontrolled industrial and municipal wastewater inputs around the periphery, dumping of wastes (including radioactive substances and solid wastes) into open parts of the sea, and accidental and operational releases of oil. Introduction of a jellyfish-like animal (*Mnemiopsis leidyi*), and overfishing have added further complications to the problem. At the beginning of the 1960s, total inorganic nitrogen, phosphate and silicate input from the Danube was 140 kt yr⁻¹, 12 kt yr⁻¹, and 790 kt yr⁻¹, respectively (Almazov, 1961). Three decades later, the Sulina branch of the Danube (one of its three main branches) alone discharged 800 kt yr⁻¹ of total inorganic nitrogen, 32 kt yr⁻¹ phosphate, and 1500 kt

yr⁻¹ silicate into the Black Sea (Cociasu et al., 1996). The total sediment load into the basin from the rivers around the periphery is about 145 million ton yr⁻¹, 65% of which enters into the northwestern shelf region (Hay, 1994). The Turkish rivers together contribute only 20% of the total sediment load (Hay, 1994). As a result, a major part of the Black Sea, particularly its northwestern shelf region, has become critically eutrophic and hypoxic (Zaitsev and Mamaev, 1997; Lancelot et al., 2002a). The exploitation of resources has been unsustainable during the last few decades as a result of dramatic reduction in fish stocks and falling recruitment.

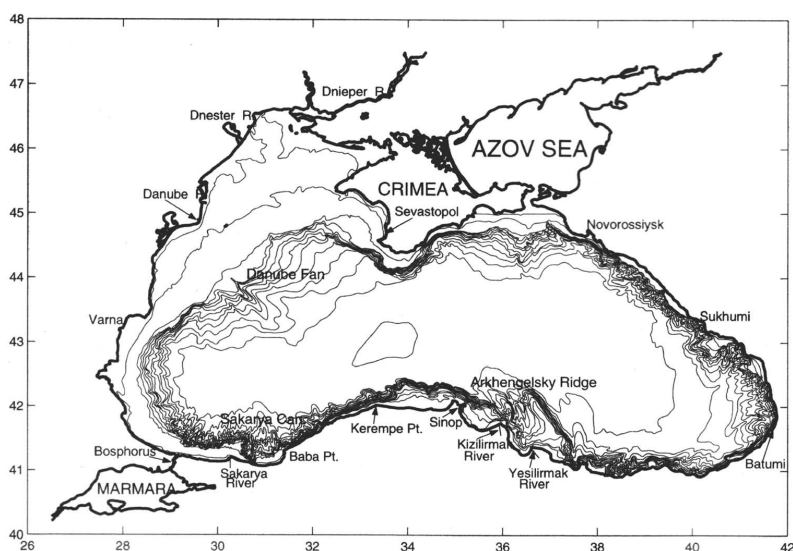


Figure 33.1 The Black Sea: geographic setting, main rivers and bathymetric features (from Besiktepe et al., 2001).

The last decade has introduced a new era in Black Sea oceanography because of collaborative research and management programs developed by the riparian states, and supported by various international organizations. They were aimed to address environmental and socio-economic issues facing the region, and to explore oceanographic characteristics of this relatively unknown, and in many respects, challenging sea. The present paper provides an overview of recent advances achieved within the framework of these efforts. Sections 2 and 3 outline the physical characteristics including the topography, water budget, and stratification, as well as major features of the upper layer horizontal circulation, respectively. This is followed in section 4 by description of the vertical biogeochemical characteristics of the upper layer water column up to the anoxic interface. This section also covers a brief overview of biogeochemical exchanges with the atmosphere. In Section 5, paleoceanographic characteristics are presented with special emphasis on connection of the Black Sea to the Aegean Sea, and sediment geochemical characteristics. Section 6 deals with major changes that took place in Black Sea ecosystem characteristics since 1970s. An overview of interdisciplinary modeling efforts is then provided in section 7. Conclusions are provided in section 8.

2. Physical Characteristics

The Black Sea, with a surface area of 423,000 km², is approximately one-fifth of the surface area of the Mediterranean. It has a total volume of 547,000 km³, and a maximum depth of around 2200 m. It contains narrow shelves and very strong topographic variations around its periphery (Fig. 33.1). The northwestern shelf (NWS), occupying ~20% of the total area, is the only major shelf region with discharges from three of Europe's largest rivers: Danube, Dniepr and Dniestr. In the north, the sea is connected to the shallow Sea of Azov by the Kerch Strait. At its southwestern end, it communicates with the Aegean basin of the Mediterranean Sea through the Sea of Marmara and the Bosphorus and Dardanelles Straits. The Black Sea has always been a basin with a positive water balance. According to the data presented by Unluata et al. (1989) (see also Ozsoy and Unluata, 1997), the sum of fluxes due to precipitation (~300 km³ yr⁻¹) and runoff (~350 km³ yr⁻¹) exceeds that of evaporation (~350 km³ yr⁻¹). The freshwater excess of 300 km³ yr⁻¹ is balanced by the net outflow through the Bosphorus defined as the difference between the transports of its two layers. This particular net transport value agrees well with the estimates for 1980s and 1990s obtained by long-term hydrological-meteorological data (Peneva et al., 2001). It is also found to be consistent with the net Bosphorus transport computed independently by means of a two layer hydrodynamic Bosphorus model (Oguz et al., 1990a).

Today, the intermediate and deep water masses below a permanent halocline at depths of 100–150 m possess almost vertically uniform characteristics defined by $T \sim 9^\circ\text{C}$, $S \sim 22$, $\sigma_t \sim 17.0 \text{ kg m}^{-3}$ (Murray et al., 1991). The deepest part of the water column covering the entire abyssal plain of the sea, approximately below 1700m, involves a vertically homogeneous and horizontally uniform water mass formed during several thousands of years by convective mixing due to the geothermal heat flux of about 40 W m^{-2} from the bottom (Murray et al., 1991). The physical characteristics of the Mediterranean underflow, including its volume, velocity, temperature and salinity, are modified considerably by mixing with the upper layer waters as they cross the shelf (Oguz and Rozman, 1991; Latif et al., 1991; Murray et al., 1991; Ozsoy et al., 1993, 2001; Di Iorio and Yuce, 1998; Gregg and Ozsoy, 1999). The effluent issuing from the Bosphorus is first transported in a narrow channel, and then enters the shelf with typical values of $T \sim 12\text{--}13^\circ\text{C}$ and $S \sim 30$. It follows persistently a north-northwestward track regulated by the small scale topographic variations in the shelf (Latif et al., 1991; Ozsoy et al., 2001), spreads out as a thin layer along the bottom of the shelf, and becomes highly diluted by entrainment of relatively colder and less saline ambient waters of the Cold Intermediate Layer (CIL) origin. The modified Mediterranean water is then injected through intrusions at intermediate depths in the form of multiple layers extending towards the interior from the continental slope (Oguz et al., 1990b; Murray et al., 1991; Ozsoy et al., 2002; Konovalov et al., 2003). Signature of the Mediterranean inflow within the interior parts of the basin is best monitored within the uppermost 500 m depth (Ozsoy et al., 1993), where the residence time of the sinking plume varies from ~10 years at 100 m depth to ~400 years at 500 m (Ivanov and Samodurov, 2001; Lee et al., 2002).

The density within the upper 100 m layer changes seasonally as much as $\sigma_t \sim 3\text{--}4 \text{ kg m}^{-3}$. In winter, the northwestern shelf and near-surface levels on top of the

thermohaline domes of the cyclonic cell exhibit vertically uniform conditions in response to strong atmospheric cooling, evaporation and intensified wind mixing associated with a succession of strong, cold and dry continental wind events. The upper layer, homogenized up to ~ 50 m depth, is identified by $T \sim 5\text{--}6^\circ\text{C}$, $S \sim 18.5\text{--}18.8$ and $\sigma_t \sim 14.5 \text{ kg m}^{-3}$ (Oguz et al., 1990b; Krivosheya et al., 2002). As the spring warming stratifies the surface water, the convectively generated cold water remains confined below the seasonal thermocline, and forms the CIL of the thermohaline structure. The summer mixed layer with depths less than 20 m has typical characteristics of $T \sim 25^\circ\text{C}$, $S \sim 18$ and $\sigma_t \sim 10.0\text{--}11.0 \text{ kg m}^{-3}$.

The water and salt budget calculations for the Bosphorus-Black Sea system, represented in the form of a two-layer box for the Bosphorus, two boxes for the interior basin and the western shelf in the upper layer, and two boxes representing the Bosphorus-Black Sea junction region and the interior basin in the lower layer (Fig. 33.2), suggest that a surface outflow of $\sim 604 \text{ km}^3 \text{ yr}^{-1}$ exits from the basin through the Bosphorus. It comprises $54 \text{ km}^3 \text{ yr}^{-1}$ coastal flow of fresh water origin along the western shelf with salinity 16.5, and $550 \text{ km}^3 \text{ yr}^{-1}$ from the rest of the basin with an average salinity of 18. In return the denser Mediterranean water with the average salinity of 35.5 enters into the Bosphorus-Black Sea junction region as an underflow at a rate of $304 \text{ km}^3 \text{ yr}^{-1}$. There, the Mediterranean plume with salinity of 26.5 entrains the upper layer flow of $426 \text{ km}^3 \text{ yr}^{-1}$ from the CIL to form a total transport of $730 \text{ km}^3 \text{ yr}^{-1}$ flowing into deeper parts of the lower layer of the basin interior having an average salinity of 22. This input is balanced by the difference of downward and upward fluxes of 639 and $1369 \text{ km}^3 \text{ yr}^{-1}$, respectively, across the interface between the upper and lower layers.

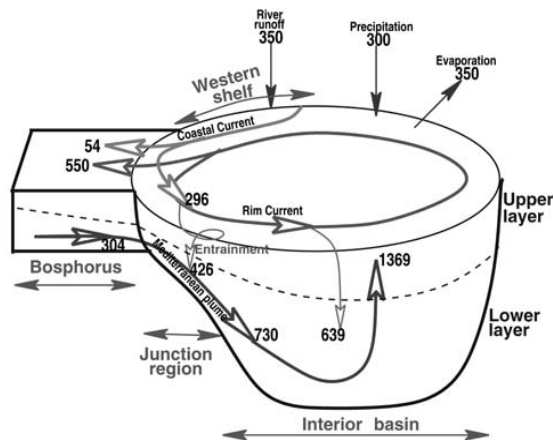


Figure 33.2 Schematic view of the five compartment box model representation of the Black Sea, and main intercompartmental fluxes computed by the water and salt budgets.

The upper layer water column was subjected to considerable climate-induced warming during the 1990s (Oguz et al., 2003). The basin-averaged winter-mean (December-March) sea surface temperatures (SSTs) derived from a 9 km monthly-

mean AVHRR data set for regions deeper than 200 m suggested relatively uniform values of 8.1 ± 0.3 °C from 1985 to 1991. They were followed by a strong cooling phase in 1992–1993 with the minimum SST value of 6.8 °C, and subsequently by the 1994–1996 strong winter warming phase with ~ 2 °C rise in the SST (Fig. 33.3a). The winter warming continued at a more gradual level after 1996. The warmer winter SSTs were related to weaker heat loss to the atmosphere, and weaker wind stress forcing exerted on the sea surface (Nezlin, 2001). The cooling-warming cycle seen in the AVHRR winter-mean SST data was supported by a similar cycle in the winter-mean air and SST temperatures (Fig. 33.3b) measured near Novorossik located along the northeastern coast of the Black Sea (Titov, 2000; Krivosheya et al., 2002). The annual-mean SST variations, also depicted in Fig. 33.3a, suggest warming of the Black Sea surface waters in the form of a linear trend with temperatures rising from ~ 14.2 °C in 1993 to ~ 16.4 °C in 2001. The upper layer stratification and circulation characteristics were modified subsequently by gradual depletion of the CIL (Staneva and Stanev, 2002; Krivosheya et al., 2002), rising of the mean winter sea level and accompanying weakening of the basinwide cyclonic circulation system (Stanev and Peneva, 2002), as well as ~ 10 m rise of the $\sigma_t \sim 16.2$ kg m⁻³ isopycnal surface characterizing the position of the anoxic interface (Yakushev et al., 2001).

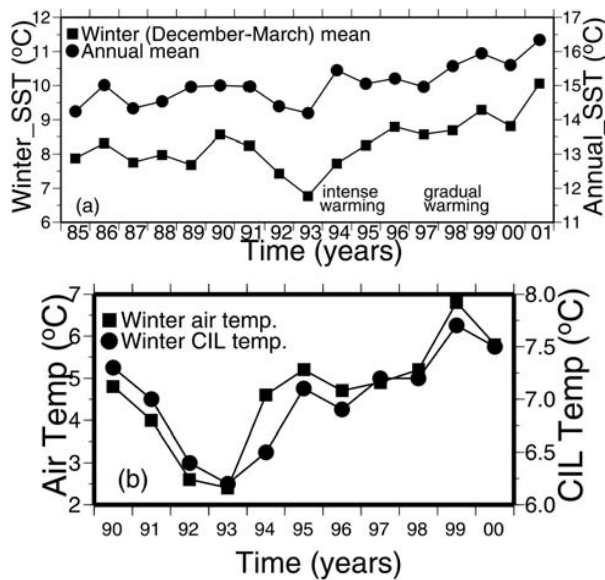


Figure 32.3 (a) The basin-averaged, winter (December-March)-mean (squares) and annual-mean (dots) AVHRR sea surface temperature distributions in the Black Sea from 1985 to 2001. The data are obtained by 9 km monthly-mean gridded AVHRR Oceans Pathfinder data set. The basin-averaging excludes the shelf areas shallower than 200 m (redrawn from Oguz et al., 2003), (b) the winter-mean air temperature (squares) and surface mixed layer temperature (dots) near Novorossik along the northeastern coast of the Black Sea.

3. Circulation characteristics

The upper layer waters of the Black Sea are characterized by a predominantly cyclonic, strongly time-dependent and spatially-structured basinwide circulation. Many details of the circulation system have been explored using recent hydrographic data (Oguz et al., 1993, 1994, 1998; Oguz and Besiktepe, 1999; Gawarkiewicz et al., 1999; Krivosheya et al., 2000), AVHRR data (Oguz et al., 1992; Sur et al., 1994, 1996; Sur and Ilyin, 1997; Ginsburg et al., 2000, 2002a; Afanasyev et al., 2002; Zatsepin et al., 2003), altimeter data (Korotaev et al., 2001 and 2003; Sokolova et al., 2001), and CZCS and SeaWIFS data (Ozsoy and Unluata, 1997; Oguz et al., 2002a; Ginsburg et al., 2002b). These analyses reveal a complex, eddy-dominated circulation with different types of structural organizations within the interior cyclonic cell, the Rim Current flowing along the abruptly varying continental slope and margin topography around the basin, and a series of anticyclonic eddies in the onshore side of the Rim Current. The interior circulation comprises several sub-basin scale gyres, each of them involving a series of cyclonic eddies. They evolve continuously by interactions among each other, as well as with meanders, and filaments of the Rim Current. The Rim Current structure is accompanied by coastal-trapped waves with an embedded train of eddies and meanders propagating cyclonically around the basin (Sur et al., 1994; Sur et al., 1996; Oguz and Besiktepe, 1999; Krivosheya et al., 2000; Ginsburg et al., 2002a,b). Over the annual time scale, westward propagating Rossby waves further contribute complexity to the basinwide circulation system (Stanev and Rachev, 1999). According to the Acoustic Doppler Current Profiler measurements (Oguz and Besiktepe, 1999), the Rim Current jet has a speed of 50–100 cm/s within the upper layer, and about 10–20 cm/s within the 150–300 m depth range. The mesoscale features evolving along the periphery of the basin as part of the Rim Current dynamic structure apparently link coastal biogeochemical processes to those beyond the continental margin, and thus provide a mechanism for two-way transports between nearshore and offshore regions. Taking the relatively narrow width of the basin into account, such mesoscale processes can easily give rise to meridional transports from one coast to another.

Apart from complex eddy-dominated features, larger scale characteristics of the upper layer circulation system possess a distinct seasonal cycle, as suggested by objectively analyzed, optimally interpolated and dynamically assimilated sea level anomaly data provided by the Topex-Poseidon and ERS-1/2 altimeters period from 1 January 1993 to 31 December 1998 (Korotaev et al., 2003). As shown by the model-derived circulation patterns (Fig. 33.4) for the middle of February, July and October, the interior cyclonic cell in winter months involves a two-gyre system surrounded by a rather strong and narrow peripheral jet without any appreciable lateral variations (Fig. 33.4a). This system transforms into a multi-centered composite cyclonic cell surrounded by a broader and weaker Rim Current zone in summer (Fig. 33.4b). The interior basin flow field further weakens and finally disintegrates into smaller scale cyclonic features in autumn (Fig. 33.4c). A composite peripheral current system is hardly noticeable in this season (Afanasyev et al., 2002). The turbulent flow field is, however, rapidly converted into a more intense and organized structure after November-December.

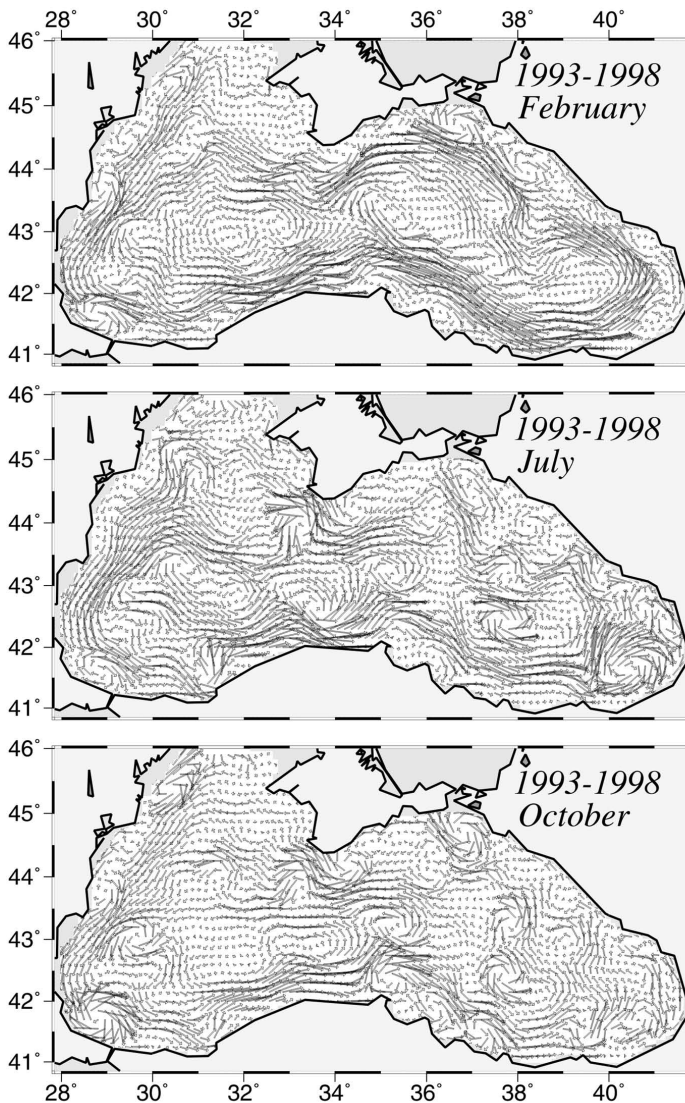


Figure 33.4 The upper layer circulation maps for (a) mid-February, (b) mid-July, (c) mid-October, constructed by the six year (1993–1998) averaging of the daily circulation fields computed by assimilating the Topex-Poseidon and ERS-I,II altimeter data into a 1.5 layer reduced gravity model described by Korotaev et al. (2003).

The most notable quasi-persistent and/or recurrent features of the circulation system, as schematically presented in Fig. 33.5, include (i) the meandering Rim Current system cyclonically encircling the basin, (ii) two cyclonic sub-basin scale gyres comprising four or more gyres within the interior, (iii) the Bosphorus, Sakarya, Sinop, Kizilirmak, Batumi, Sukhumi, Caucasus, Kerch, Crimea, Sevastopol, Danube, Constantza, and Kaliakra anticyclonic eddies on the coastal side of the Rim Current zone, (iv) bifurcation of the Rim Current near the southern tip of the

Crimea; one branch flowing southwestward along the topographic slope zone, and the other branch deflecting first northwestward into the shelf and then contributing to the southerly inner shelf current system, (v) convergence of these two branches of the original Rim Current system near the southwestern coast, (vi) presence of a large anticyclonic eddy within the northern part of the northwestern shelf.

The basic mechanism which controls the flow structure in the surface layer of the northwestern shelf is spreading of the Danube outflow. Wind stress and Rim Current structure along the offshore side of the shelf are additional modifiers of this system. The freshwater discharge influences not only the circulation and mixing properties, but also the ecosystem of the entire shelf region along the western coast. The Danube plume generally forms an anticyclonic bulge confined within the upper 25 m layer. The leading edge of this plume protrudes southward (i.e. downstream) as a thin baroclinic boundary current along the western coastline. The coastal jet is separated from the interior waters by a well defined front with salinity differences of more than 3.0 over an approximately 50 km zone along the coast. It is often unstable, exhibits meanders and spawns filaments, which extend across the wide topographic slope zone. The shelf and interior waters undergo cross-shelf exchanges as reported consistently in hydrographic surveys, satellite imagery, and altimeter data. An anticyclonic circulation system accompanying with small-scale structures over the northwestern shelf, shown in Fig. 33.5, have also been reproduced by modeling studies (e.g. Oguz et al., 1995; Staneva et al., 2001; Beckers, et al., 2002).

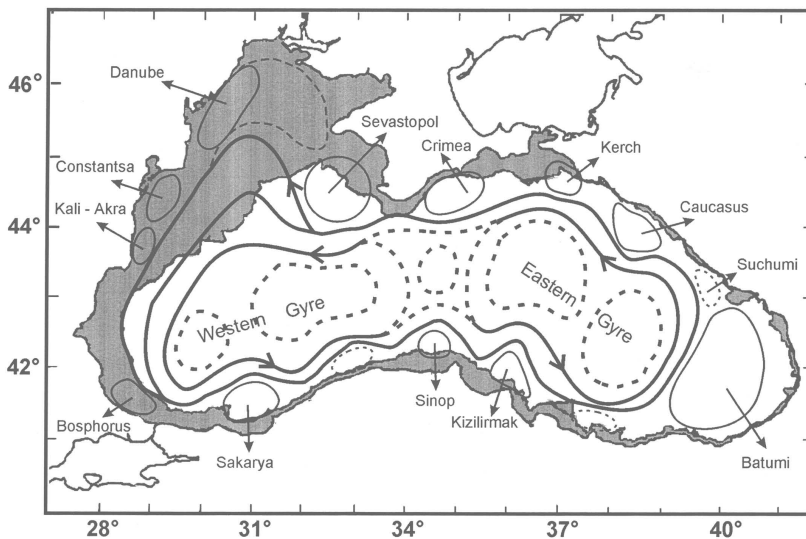


Figure 33.5 The schematic diagram showing major quasi-permanent/recurrent features of the upper layer circulation identified by synthesis of hydrographic studies and analysis of the Topex-Poseidon and ERS-I,II altimeter data.

4. Major features of the vertical biogeochemical structure

4.1 Nutrient and organic matter characteristics

The upper layer biogeochemical structure overlying the deep and lifeless anoxic pool (except anaerobic bacteria) involves four distinct layers. The uppermost part from the free surface to the depth of 1% light level is covered by a shallow euphotic zone with a maximum thickness of nearly 50 m. This is the layer of active planktonic processes (e.g uptake, grazing, mortality, microbial loop, etc.), and is characterized by high oxygen concentrations on the order of 300 μM as well as seasonally varying nutrient and organic material concentrations supplied laterally from rivers and vertically from sub-surface levels through vertical mixing. In the interior basin, the surface mixed layer waters are poor in nutrients for most of the year except for occasional incursions from coastal regions, and by wet precipitation. Below the seasonal thermocline and in the deeper part of the euphotic zone, nitrate concentrations increase due to their recycling as well as continuous supply from the nutricline. Nitrate accumulation in this light-shaded zone generally supports summer subsurface phytoplankton production (Oguz et al. 2000). In winter, nutrient stocks in the euphotic zone waters are renewed from the nutricline depths through upwelling, vertical diffusion and seasonal wind and buoyancy-induced entrainment processes, and depleted by biological utilization. About 90% of the sinking particles are remineralized inside the euphotic zone and the subsequent 20–30 m part of the oxygenated, aphotic zone (the so-called “upper nitracline” zone) where nitrate concentrations increase up to $\sim 8 \mu\text{M}$ at ~ 70 – 80 m in cyclonic regions, and are re-supplied back to the surface waters to refuel the biological pump. Only a small fraction of particulate matter sinks to the deeper anoxic part of the sea (Lebedeva and Vostokov, 1984; Karl and Knauer, 1991), which occupies the water column below ~ 100 m depth within the interior parts and ~ 200 m in the onshore, anticyclonically-dominated side of the Rim Current. This loss is compensated by lateral nitrogen input mainly from the River Danube (Cociasu et al., 1996), by wet deposition and nitrogen fixation. The nutrient fluxes of anthropogenic origin are transported across the shelf and around the basin through the Rim Current system, and supplied ultimately to the interior basin, and some of which is lost in the form of Bosphorus surface flow in winter months (Polat and Tuğrul, 1995). The river supply in the NWS gives rise to a high N/P ratio within the shallow water column, and further constitutes a major source of selectively nitrate-enriched CIL in winter. The river influence markedly weakens toward the south along the coast and offshore for most of the year due to photosynthetic consumption of dissolved inorganic nutrients. Nevertheless, below the seasonal thermocline, the thicker CIL in coastal regions contains measurable concentrations of nitrate but very low ($<0.02 \mu\text{M}$) phosphate values, yielding abnormally high N/P ratios (Codispoti et al., 1991; Basturk et al., 1998a).

When nitrate profiles are plotted against density, the position of the peak concentration coincides approximately with the $\sigma_t \sim 15.5 \text{ kg m}^{-3}$ level (Fig. 33.6a) (Tuğrul et al., 1992; Saydam et al., 1993; Basturk et al., 1994; Yilmaz et al., 1998a), although some degree of variability in its position between $\sigma_t \sim 15.3$ and 15.6 kg m^{-3} isopycnal surfaces as well as in its maximum concentrations from 6 to 10 μM are observed in the data (Basturk et al., 1998a; Oguz et al., 2000). The nitrate structure is accompanied by occasional peaks of ammonium on the order of 0.5 μM near the

base of the euphotic zone due to inputs from excretion and aerobic organic matter decomposition following subsurface plankton production. Ammonium concentrations are then subject to a linear trend of decrease towards trace concentrations at the anoxic interface (Basturk et al., 1998a). Within the oxygen deficient part of the water column below $\sigma_t \sim 15.6 \text{ kg m}^{-3}$, organic matter decomposition proceeds via denitrification. This results in formation of the “lower nitracline” zone with sharp decrease of nitrate concentrations at a thickness of about 30–40 m from their peaks to their trace values around 100 m depth or $\sigma_t \sim 16.0 \text{ kg m}^{-3}$ isopycnal surface (Fig. 33.6a). Nitrate consumption due to oxidation of reduced manganese and ammonium may also contribute to reduction of nitrate concentrations within the lower part of the suboxic zone (Murray et al., 1995). Importance of the Anammox type reactions ($\text{NO}_2^- + \text{NH}_4^+ \rightarrow \text{N}_2$) in the Black Sea was recently shown by Kuypers et al. (2003). In these processes, bacteria utilize nitrate and nitrite ions to oxidize organic matter, reduced manganese and ammonium. The nitrate is then reduced to nitrogen gas with nitrite as an intermediate product. A nitrite peak with concentrations up to $0.5 \mu\text{M}$ is usually observed at $\sigma_t \sim 15.85 \pm 0.05 \text{ kg m}^{-3}$ located approximately 10 m (or, equivalently, $\sigma_t \sim 0.1 \text{ kg m}^{-3}$) above the position of the zone of nitrate depletion (Fig. 33.6a). This coincides with the position of the phosphate minimum (Fig. 33.6b) (Codispoti et al., 1991). The thickness of the nitrite peak therefore marks the denitrification zone. The deep sulphide-bearing waters in the Black Sea contain no measurable nitrate, but constitute large pools of ammonium and dissolved organic nitrogen. Reduction in subsurface nitrate concentrations, however, does not appreciably limit primary production since the euphotic zone and extent of the winter mixed layer always lie above its maximum concentration zone.

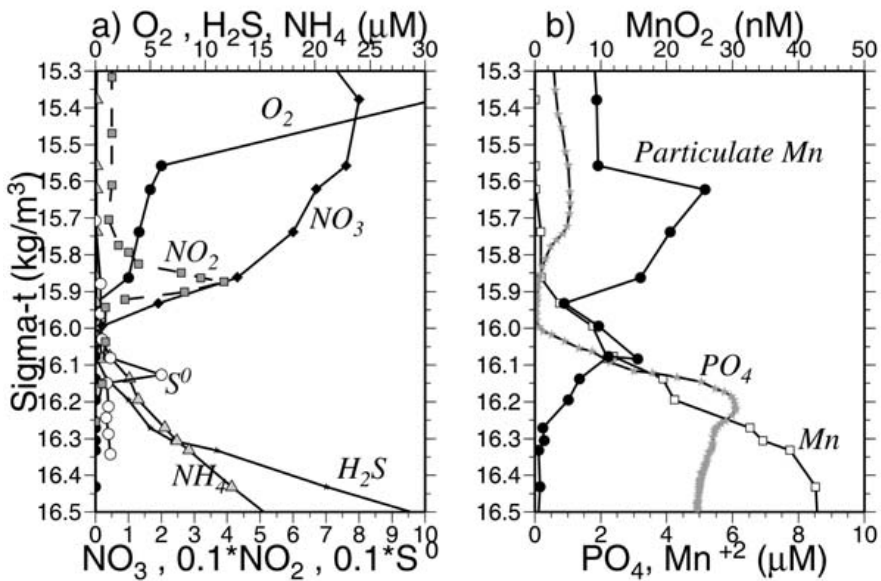


Figure 33.6 (a) Depth profile of density for the upper 150 m water column, (b) O_2 , HS^- , NH_4^+ , NO_3^- , NO_2^- , S^0 profiles, and (c) MnO_2 , Mn , PO_4 profiles plotted versus density (σ_t) at station 43°N , 34°E during RV Knorr survey of 13 June 1988 (from Oguz et al., 2001a).

The vertical structure of phosphate concentrations resembles that of nitrate in the upper layer but is quite complicated in the suboxic/anoxic layers (Fig. 33.6b). Phosphate concentrations increase gradually within the deeper part of the euphotic layer and the upper nitracline zone up to a maximum value of 1.0–1.5 μM around $\sigma_t \sim 15.6 \text{ kg m}^{-3}$, and then decreases to minimum of about 0.05–0.1 μM in the suboxic zone around $\sigma_t \sim 15.9 \pm 0.1 \text{ kg m}^{-3}$ where nitrite locally displays a peak in the cyclonic basin (Codispoti et al., 1991; Tugrul et al., 1992; Murray et al., 1995). It then increases abruptly to peak values of 5.0–8.0 μM near $\sigma_t \sim 16.2 \text{ kg m}^{-3}$ coinciding with the first appearance of sulfide in the water column. The formation of this peak has been explained by dissolution of phosphate-associated iron and manganese oxides (Shaffer, 1986; Codispoti et al., 1991). Silicate possesses a relatively simpler vertical structure with a steady increase of concentrations below the euphotic layer up to about 70–75 μM at $\sigma_t \sim 16.2 \text{ kg m}^{-3}$ defining the anoxic boundary in the open sea, and then to about 150 μM at the depth of $\sigma_t \sim 16.8 \text{ kg m}^{-3}$ in the upper anoxic water.

A major contribution to total organic carbon (TOC) in the Black Sea comes from its dissolved form (DOC) (Sorokin, 2002; Tugrul, 1993). Both DOC and slowly sinking suspended particulate organic matter (SPOM) are especially abundant within the NWS waters due to large, river-borne organic matter and nutrient input. Their concentrations in the surface layer of the western central basin is 160–250 μM for DOC (Tugrul, 1993; Polat and Tugrul 1995), and from 60–80 μM to $\sim 10 \mu\text{M}$ for POC (Burlakova et al., 1997; Coban-Yldz et al., 2000a,b). The riverine supply alone contributes around 130 μM of the total DOC content within surface waters, and the rest represents contribution from local biological production. The DOC concentration decreases steadily with depth to background values of 110–130 μM within the oxic/anoxic interface and further below to the bottom (Tugrul, 1993). Various references however have reported different DOC concentrations, such as from $\sim 300 \mu\text{M}$ at the surface to $\sim 265 \mu\text{M}$ at 100m and $\sim 190 \mu\text{M}$ near the bottom (Sorokin, 2002), or from 100 μM at the surface to $\sim 60 \mu\text{M}$ in the suboxic-anoxic interface zone (Karl and Knauer, 1991). SPOM concentrations also decrease towards lower levels of $\sim 2\text{--}3 \mu\text{M}$ for particulate organic carbon (POC) in the suboxic zone. At the suboxic/anoxic transition zone, SPOM exhibits a small maximum (POC $> 10 \mu\text{M}$) probably due to bacterially-mediated redox reactions (Coban-Yldz et al., 2000a,b, 2003). The peak is more distinguishable at the shelf-break regions of the southwestern Black Sea possibly due to additional supply of chemical energy through lateral injection from the Bosphorus plume. During productive periods, the C/N ratio of SPOM within the surface layer is similar to the Redfield ratio. The C/N ratio in the surface layer, however, increases during less productive periods (i.e. summer-autumn) due to selective decay of nitrogenous compounds. The ratio then decreases to the Redfield value towards the suboxic/anoxic transition zone, in accordance with increasing SPOM concentrations. Despite distinct seasonal and regional variations in SPOM and chlorophyll concentrations, the isotopic compositions of carbon ($\delta^{13}\text{C}$) and nitrogen ($\delta^{15}\text{N}$) in SPOM stay nearly vertically uniform within the euphotic zone (Calvert and Fontugne, 1987; Fry et al., 1991; Kodina et al., 1996; Coban-Yldiz et al., 2003). At deeper levels, $\delta^{15}\text{N}$ increases as $\delta^{13}\text{C}$ decreases in the upper nitracline zone; $\delta^{15}\text{N}$ values initially increase from 3–4.5‰ to around 7.2 to 9.1‰ at the depth of the

nitrate maximum then decrease to a minimum of 2.0 ‰ within the anoxic interface of the interior basin (Coban-Yildiz et al., 2003).

4.2. Suboxic layer and suboxic-anoxic interface zone characteristics

The euphotic layer oxygen concentration undergoes pronounced seasonal variations within a broad range of values from about 250 to 450 μM . The period from the beginning of January until mid-March exhibits vertically uniform mixed layer concentrations of $\sim 300\text{--}350$ μM , ventilating the upper ~ 50 m of the water column as a result of convective overturning. The rate of atmospheric oxygen input in the ventilation process is proportional to the excess of saturated oxygen concentration over the surface oxygen concentration. The maximum contribution of oxygen saturation is realized towards the end of February during the period of coolest mixed layer temperatures, coinciding with the maximum and deepest winter oxygen concentrations during the year. After March, initiation of the warming season is accompanied by oxygen loss to the atmosphere, thus reducing oxygen concentrations within the uppermost 10 m to 250 μM during the spring and summer months. A subsequent linear trend of increase across the seasonal thermocline links low near-surface oxygen concentrations to those of relatively higher sub-thermocline concentrations. Depending on the strength of summer phytoplankton productivity, the sub-thermocline concentrations exceed 350 μM in summer. Irrespective of the season, the oxygen concentration then decreases almost linearly within the upper nitracline zone to concentrations of about 100 μM at $\sigma_t \sim 15.3$ kg m^{-3} and about 10 μM at $\sigma_t \sim 15.6$ kg m^{-3} due to intense oxygen consumption during the decomposition process of organic matter. Oxygen concentrations vanish completely near the anoxic interface located at $\sigma_t \sim 16.2$ kg m^{-3} (Fig. 33.6a).

The oxygen deficient ($\text{O}_2 < 10$ μM), non-sulfidic layer having a thickness of 10-to-40 m coinciding with the lower nitracline zone is more commonly referred to as the "Suboxic Layer (SOL)". It has been identified for the first time by Murray et al. (1989, 1991). Earlier observations generally measured dissolved oxygen concentrations more than 10 μM inside the sulfidic layer (Sorokin, 1972; Faschuk, et al., 1990; Rozanov et al., 1998). Grashoff (1975) was the first to point out that co-existence of dissolved oxygen and H_2S was probably an artifact of atmospheric contamination during sampling. More recent observations (Tugrul et al., 1992; Saydam et al., 1993; Buesseler et al., 1994; Ereemeev, 1996; Basturk et al., 1994, 1998a; Konovalov et al., 2003) have supported existence of the SOL along the density surfaces of $\sigma_t \sim 15.55 \pm 0.05$ and 16.15 ± 0.05 kg m^{-3} . Analyzing the data available since the 1960s, Tugrul et al. (1992), Buesseler et al. (1994) and Konovalov and Murray (2001) showed that the suboxic zone was in fact present earlier than its first observation in 1988, but it was masked because of low sampling resolution and contamination of water samples with atmospheric oxygen.

Below the suboxic zone is the deep anoxic layer containing high concentrations of hydrogen sulphide and ammonium. The boundary between the suboxic and anoxic layers is the site of a series of complicated redox processes (Murray et al., 1995; Rozanov, 1996). As dissolved oxygen and nitrate decrease towards zero concentrations at the suboxic-anoxic interface, dissolved manganese, ammonium and hydrogen sulfide begin to increase at the interface (Fig. 33.6a,b). Marked gradients of particulate manganese around this transition zone near $\sigma_t \sim 16.0$ kg m^{-3}

(Fig. 33.6b) reflect the role of manganese cycling as proposed by Spencer and Brewer (1971), Brewer and Spencer (1974), Kempe et al. (1991), Tebo (1991), Tebo et al. (1991), Lewis and Landing (1991), and Oguz et al. (2001a). The deep ammonium, sulfide and manganese pools have accumulated as a result of organic matter decomposition within the last 5000 years, after the Black Sea was converted into a two-layer stratified system. The ammonium concentrations, increasing sharply below $\sigma_t \sim 16.0 \text{ kg m}^{-3}$, reach at values of $10 \mu\text{M}$ at 150 m ($\sigma_t \sim 16.5 \text{ kg m}^{-3}$) and $20 \mu\text{M}$ at 200 m ($\sigma_t \sim 16.8 \text{ kg m}^{-3}$). The gradient of ammonium profiles in the vicinity of the suboxic-anoxic interface implies that no ammonium is supplied to the photic zone from the anoxic region.

As pointed out above, major characteristic features of the Black Sea vertical biogeochemical structure are customarily expressed in terms of density used as the vertical coordinate. The assumption of isopycnal uniformity and independence of biogeochemical properties from the circulation features was first suggested by Vinogradov and Nalbandov (1990). It was then supported by Tugrul et al. (1992) and Saydam et al. (1993) when the oxygen, sulfide, and nutrient profiles from the 1988 Knorr and 1991 Bilim surveys were plotted all together against density. Because most of the data taken in these surveys covered the interior basin characterized by a similar type of cyclonic circulation system, this assertion was found to be reasonably valid. More recently, re-analysis of historical data together with model simulations (Oguz, 2002) noted some differences in different parts of the sea. This implies sensitivity of the vertical biogeochemical structure to local circulation characteristics and subsequently to the direction and intensity of vertical diffusive and advective fluxes within the water column. The vertical variations therefore can not be expressed in terms of density without taking into account physical characteristics of the water column. For example, as shown in Fig. 33.7, the upper boundary of the SOL in the eastern Black Sea defined by the position of $10 \mu\text{M}$ oxygen concentration markedly varies from $\sigma_t \sim 15.55 \pm 0.1 \text{ kg m}^{-3}$ in the cyclonic gyre (centered at 42.3°N , 38.5°E) to $\sigma_t \sim 15.9 \pm 0.1 \text{ kg m}^{-3}$ in the adjacent anticyclone (centered at 41.8°N , 40.2°E) during September 1991 (Oguz et al., 1994). The anticyclonic nature of the latter region implies a more pronounced downward oxygen transport resulting in a narrower SOL.

The anaerobic sulfide oxidation and nitrogen transformations coupled to the manganese and iron cycles have been considered one of the mechanisms to maintain stability of the interface structure between the suboxic and anoxic layers (Murray et al., 1995; 1999). The upward fluxes of sulfide and ammonium are oxidized by Mn(III, IV) and Fe(III) species, which are generated by Mn(II) and Fe(II) oxidation by reactions with nitrate. The upward flux of ammonium is also consumed by $\text{NO}_3^-/\text{NO}_2^-$ via anammox reaction (Murray et al., 1995; Kuypers et al., 2003). These oxidation-reduction reactions are microbially catalyzed, but dissolved chemical reduction may also play a role in Mn(IV) reduction with sulfide. Modeling studies (Oguz et al., 2001a) demonstrate that this mechanism alone could provide the observed redox structure. Anaerobic photosynthesis is considered an additional mechanism contributing to the SOL formation. The reduced chemical species (HS^- , Mn^{2+} , Fe^{2+}) are oxidized by anaerobic phototrophic bacteria in association with phototrophic reduction of CO_2 to form organic matter. This mechanism was supported by the discovery of large quantities of bacteriochlorophyll pigments near the suboxic-anoxic boundary (Repeta et al., 1989; Repeta and Simp-

son, 1991; Jorgensen et al., 1991; Jannasch et al., 1991). A particular bacterium is capable of growth using reduced S (H_2S or S^0) at very low light levels ($\ll 0.1\%$ of the incident radiation at the surface). The third mechanism is oxidation of H_2S by oxygen and particulate manganese injected horizontally into the anoxic layer (Murray et al., 1989; Tebo et al., 1991; Basturk et al., 1998a). Konovalov and Murray (2001) show that more than 50% of the upward flux sulfide could be consumed by this pathway.

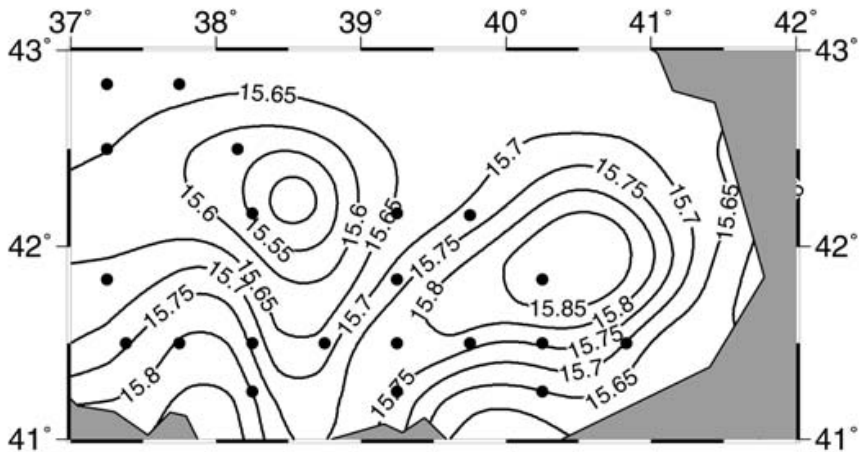


Figure 33.7 Horizontal distributions of σ_t (kg m^{-3}) at the depth of $10 \mu\text{M}$ oxygen concentration obtained from measurements of RV Bilim 1991 survey in the southeastern part of the Black Sea. Station locations are shown by dots. (redrawn from Oguz, 2002).

It is difficult to quantify the anoxygenic photosynthesis as a mechanism of basin-wide relevance. Its contribution must be limited to cyclonic regions where the anoxic interface zone is shallow enough to be able to receive sufficient light to maintain bacterial photosynthetic activity. Presence of a persistent suboxic zone structure with its lower boundary located at depths of around 160–180 m within the quasi-permanent anticyclonic gyre of the eastern basin (Basturk, et al. 1998a) therefore suggests that anaerobic sulfide oxidation should control first-order dynamics of the redox structure in the Black Sea. Anaerobic photosynthesis is expected to have an additional contribution to the dissolved oxygen-hydrogen sulfide separation, and thus to formation of somewhat thicker SOL at shallower depths within cyclonic areas of the basin.

Because the sulfide layer is located only about 100 m below the surface in most parts of the Black Sea, the possible vertical extent of horizontal ventilation of the upper layer water column is a critically important issue. One possible ventilation mechanism is local convective overturning following intense winter atmospheric cooling episodes. There is, however, no data to support the ventilation of suboxic and anoxic layers through atmospheric oxygen supply. According to model simulations (Oguz et al., 2000; Oguz, 2002), episodic strong cooling events under realistic ranges of heat fluxes could only increase the density of the mixed layer up to σ_t

$\sim 15.0 \text{ kg m}^{-3}$ which corresponds to deepening of the mixed layer to about 75 m within the cyclonic regions. Thus, it seems that the strong stability of the water column hardly allows any seasonal variation of oxygen below the oxycline due to atmospheric ventilation. Oxygen supplied by the Mediterranean waters of Bosphorus origin also contributes locally to sulfide oxidation (Konovalov and Murray, 2001; Neretin et al., 2001). The effects of ventilation by the Bosphorus plume can be dramatically seen in the vertical profiles of T, S, O_2 and H_2S in the southwestern region of the Black Sea (Konovalov et al., 2003). Basturk, et al. (1998b) provided an example of the cross-shelf ventilation of the interior basin along the periphery of the Black Sea, induced by onshore-offshore exchanges of water masses due to meanders and complex eddy activities of the Rim Current system. Quasi-lateral injection of oxygen rich shelf waters offshore into a fine particle layer (Kempe et al., 1991; Rozanov et al., 1998) situated between isopycnal surfaces of $\sigma_t \sim 15.9 \text{ kg m}^{-3}$ and $\sigma_t \sim 16.4 \text{ kg m}^{-3}$ was identified by dissolved oxygen concentrations of about $20 \mu\text{M}$ within this layer.

4.3. *Biogeochemical exchanges with atmosphere*

Biologically produced gases in the surface ocean have a major impact on the global atmospheric cycling of elements such as sulfur, nitrogen and carbon, and can play an important role in the global climate system. Dimethyl sulfide (DMS) is the principal and most abundant biogenic organic sulfur compound entering the atmosphere, where it undergoes photo-oxidation and transformation to methanesulfonate (MSA) and SO_4 aerosol. In addition to anthropogenic and volcanic sources, it provides a biogenic contribution to non-sea-salt sulfate (nss-sulfate) in marine aerosols. The importance of nss-sulfate comes from its effect on the Earth's radiation budget by backscattering solar radiation to space (Charlson et al., 1991) and by controlling the formation of cloud condensation nuclei (Charlson et al., 1987). It has been suggested that its contribution to atmospheric cooling nearly compensates the estimated warming due to increased carbon dioxide and other greenhouse gases. The global oceanic contribution is about 40 % of the total sulfur burden of the atmosphere, comparable to manmade contributions (Simo, 2001). Recent studies have indicated the potential role of the Black Sea in the production of DMS (Cokacar et al., 2001; 2004), its transfer into the atmosphere, and subsequently aerosol transport processes over the region (Kubilay et al., 2002). Aerosol MSA and nss-sulfate concentrations measured in samples collected during January 1996-December 1999 at two coastal stations along the Mediterranean coast of Turkey near Erdemli and at the island Crete near Finokalia were found to be associated with (i) the presence of high level and almost continuous phytoplankton production over the entire Black Sea by means of DMS producing species (such as coccolithophorids, flagellates, etc) in response to intense eutrophication that developed within the last two decades, and (ii) the presence of a persistent northerly low level boundary layer atmospheric transport prevailing over the region.

Kubilay et al. (2002) observed a clear signature of seasonal variations of biogenically-derived nss-sulfate concentrations in the Eastern Mediterranean atmosphere from low winter to high summer values. Their summer concentrations measured at Erdemli were among the highest reported in the world. The period of their high summer concentrations correlated very well with basinwide blooming of

coccolithophorids *E. Huxleyi* in the Black Sea during June and July every year, as suggested by the SeaWIFS mean normalized water-leaving radiance data (Cokacar et al., 2004). Low-level meridional atmospheric transport carried nss-sulfate aerosols over Anatolia into the marine atmosphere of the Eastern Mediterranean Sea roughly from the end of May to the end of September. The lateral aerosol supply from the Black Sea was found to terminate after September as the direction of low level air motions was shifted preferentially to northwesterlies during the autumn and winter months.

There is growing evidence that aeolian transported materials, particularly enriched in elements of ecological concern, such as iron, nitrogen, phosphorus, trigger phytoplankton production in the oceans (Duce et al., 1991). The Black Sea is under the particular influence of long-range aeolian transport from the Sahara, Middle East, Eastern Europe and Russian mainland in the northeast. A number of case studies confirmed transport from North Africa towards the Black Sea, particularly during spring and autumn months (Kubilay et al., 2000). On the basis of measurements performed during July 1992, dust deposition provided a total nitrogen supply of 44 kt yr^{-1} , which roughly corresponded to 13% of the total inorganic nitrogen input by the Danube outflow (Kubilay et al., 1995), and thus aerosol transport is important intermittently if not on the annual time scale.

5. Paleoceanographic characteristics

During the last glacial maximum before 12,000 BP, the Black Sea, the Sea of Marmara and Aegean Sea were about 120 m below their present levels, and were therefore decoupled from each other by shallow sills of the Bosphorus and Dardanelles. Freshwater conditions used to prevail both the Black Sea and Marmara Sea whereas the Aegean Sea reflected marine conditions. With the rise of sea level after the end of glaciation, the global sea level reached the 80 m sill depth of the Dardanelles around 12,000 BP, and salty Mediterranean water started filling the Sea of Marmara, leading to the formation of a sapropel between 10,600 and 6400 BP (Cagatay, et al., 2000). The date upon which saline Mediterranean water first entered the Black Sea during the Holocene is more uncertain and indeed a controversial issue. The traditional view (Ross and Degens, 1974; Stanley and Blampied, 1999), later elaborated by Aksu et al. (1999, 2002), suggested that the Black Sea during the period from 12,000 to 9,500 BP still remained as a freshwater lake, receiving a large freshwater inflow from the receding European ice sheet through the rivers around the periphery of the basin. These factors resulted in a substantial rise of the Black Sea level from its pre-flooding depth of -120m; by ~11,000–10,000 BP, the Black Sea has risen to the Bosphorus sill depth of -40m and subsequently began to spill large volume of waters first into the Marmara Sea across the Bosphorus, and later into the Aegean Sea across the Dardanelles Strait. Evidence for this view includes the presence of a sapropel in the Sea of Marmara (Cagatay et al., 2000), studies of shelf sediments in the Black Sea (Gorur et al., 2001), westerly-oriented bedforms in the Sea of Marmara (Aksu et al., 1999), and the analysis of planktonic and benthic foraminifera (Yanko et al., 1999; Kaminski et al., 2002). Following incursions of saline Mediterranean water into the Marmara Sea after the rise of the Aegean Sea level above the Dardanelles sill depth during the period from 12,000 to 9,500 BP, the rising sea level enabled Mediterranean inflow into the

Black Sea across the Bosphorus Strait starting by 9000 BP. The saline wedge had possibly penetrated well into the strait 500–1000 yr later, and led to a gradual salination of the Black Sea, and development of a two-layer stratification and formation of anoxic conditions by perhaps 8000 BP.

On the basis of sedimentary data from the northwestern and northern shelves of the Black Sea, Ryan et al. (1997) offered an alternative and contrasting view for the timing and development of marine connection between the Black Sea and the Sea of Marmara following the last deglaciation. According to this so-called “flood hypothesis” the Mediterranean-Black Sea post-glacial connection occurred as a result of refilling of the Mediterranean basin and then flooding catastrophically into the Black Sea in less than 2 years at a flow rate of more than $50 \text{ km}^3 \text{ day}^{-1}$ during 7150 ± 100 yr BP. This hypothesis has largely been based on the rapid first appearance of euryhaline (Mediterranean) mollusks on the Black Sea shelves at $\sim 7,500$ BP. They further speculated that this flooding event was actually the reason for the migration of early Neolithic peoples from the region as mentioned in the biblical story of Noah’s flood (Ryan and Pitman, 1999). Ballard et al. (2000) identified the location of ancient beach at 155 m water depth below the present day sea surface in the south-central Black Sea, and inferred the marine flooding of the Black Sea between 7.46 and 6.82 ka by means of radiocarbon dating of mollusk shells. Ryan et al. (2003) later refined the hypothesis by considering large amounts of additional data. Aksu et al. (2002) believe that the euryhaline colonization of mollusks was not a consequence of catastrophic flooding but rather the outcome of a slow establishment of two-way flow in the Bosphorus and a time lag during which the fresher waters of the deep Black Sea were replaced by more saline inflow, eventually allowing marine organisms to colonize the Black Sea shelves. They suggested that mollusks arrived at the region about 7500 years ago when the level of salty Mediterranean water rose to the 100 m depths where mollusks thrive.

The Black Sea sediments deposited during the last 30,000 yr consist of three different environmental conditions of the Late-Quaternary history of the basin (Cagatay, 1999). At the bottom, *Unit 3* deposition during $\sim 30,000$ – $7,000$ BP is a laminated clay with a low ($\sim 15\%$) carbonate content, and signifies the fresh water environmental conditions prior to inflow of the Mediterranean water through the Bosphorus. It also includes dark laminae that are formed by high concentrations of unstable iron monosulfides. *Unit 2* is ~ 40 cm thick sapropel deposition consisting of mainly gelatinous organic matter with some coccolith remains, clays, inorganically precipitated aragonite, iron monosulfides and pyrite. Sapropels are occasionally interrupted by turbidite layers of terrigenous origin. Sapropel unit was deposited during a period of high plankton productivity after the flooding of the lacustrine Black Sea basin by the Mediterranean waters via the Bosphorus Strait at around 7000 BP and terminated around 2000–1600 BP. Prior to termination of *Unit 2* deposition, there is a period of time with intermittent coccolith invasions whose characteristics reveal some regional variability within the basin. *Unit 1* is ~ 30 cm thick coccolith mud, consisting of alternations of light- and dark-colored microlaminae. The light-colored laminae are composed mainly by calcareous coccolith remains deposited within the last 2000 yr after the invasion of the Black Sea coccolithophore *Emiliania huxleyi*. The dark laminae consist of clays and organic matter. The clay minerals include predominantly chlorite, smectite and illite with high chlorite/illite and smectite/illite ratios. Three peak periods of coccolith deposi-

tion implied by maximum carbonate concentrations occurred around 450, 1050, and 1500 BP. They match closely with the transitions from high to low sea level changes that took place in the history of the Black Sea.

6. Changes in the ecosystem characteristics since the 1970s

The last three decades of the Black Sea have been characterized by profound changes in its pelagic ecosystem. These changes were first noted in the biomass, taxonomic structure and succession of the phytoplankton community, particularly in the northwestern shelf. The natural phytoplankton annual cycle with spring and autumn maxima in biomass has been replaced by a pattern characteristic of eutrophied waters identified by several exceptional maxima- the summer one being the most pronounced. In addition to an increase in the frequency of blooms and the number of blooming species, individual blooms have become more monospecific. Diatoms, which were the most abundant group of the annual phytoplankton community structure prior to the 1970s, were replaced by more predominant blooms of dinoflagellates and coccolithophores (Moncheva and Krastev, 1997; Mikaelyan, 1997; Uysal et al., 1998). This phenomenon may have been caused by changes in the silicon to nitrogen ratio due to eutrophication as well as a reduction in the dissolved silicate load of the River Danube (Moncheva and Krastev, 1997) as a result of dam construction in the early 1970s (Humborg et al., 1997) and/or increased eutrophication within the Danube itself (Garnier et al., 2002). Average phytoplankton biomass in the northwestern shelf area increased from 1 g m^{-2} in the 1960s to 19 g m^{-2} in the 1970s and 30 g m^{-2} in the 1980s (Zaitsev and Mamaev, 1997). A similar trend with lower intensity was also reported for other parts of the basin (cf. Fig. 33.8a, and Mikaelyan, 1997; Kovalev et al. 1998). The transparency (as revealed from Secchi Disk measurements shown in Fig. 33.8b) of even open waters was decreased during the 1970s and 1980s. At first the ecosystem responded favorably to increased primary production by producing higher mesozooplankton and fish stocks during the second half of the 1970s and early 1980s (cf. Fig. 33.8c,e, and Porumb, 1989). By the mid-1980s, a five-fold decrease in total mesozooplankton biomass was observed due to their consumption by opportunistic species such as *Noctiluca scintillans*, *Aurelia aurita*, *Pleurobrachia rhodopis* and *Mnemiopsis leidyi*. The total abundance of these new organisms reached 99% of the total zooplankton wet weight (Shushkina et al., 1998; Kovalev et al, 1998; Shiganova, 1998; Kideys and Romanova, 2001). As quantified by the Flow Network Analysis (Gucu, 2002), overfishing that took place during the early phase of the eutrophication (i.e. early 1980s) may have triggered destabilization of the ecosystem and the population explosion of gelatinous species.

Increase in the population of gelatinous carnivores apparently led to increases in particulate and dissolved organic matter content in the upper layer water column. This resulted in enhanced bacterial production and more active organic matter decomposition (Lancelot et al., 2002a), which then resulted in increased oxygen deficiency within the upper nitracline-oxycline zone of the water column and more denitrification and associated nitrate consumption within the suboxic zone. Two implications of such modifications in the biogeochemical structure were broadening of the suboxic zone from its position at $\sigma_t \sim 15.9 \text{ kg m}^{-3}$ in the 1960s to $\sigma_t \sim 15.6 \text{ kg m}^{-3}$ during the 1980s, and a change in the gradient of the subsurface nitrate struc-

ture as well as upward shifting of the nitrate peak by about 10 m (Konovalov and Murray, 2001). An increase in the value of the nitrate maximum from about 2.0 mmol m^{-3} to more than 6.0 mmol m^{-3} during 20 years of nitrate accumulation in the water column was roughly equivalent to the contribution from anthropogenic nutrient load after the 1960s. The greater contribution of POM export flux to the anoxic zone led to an increase in the rate of sulfate reduction by about 15%, and thus increased sulfide concentrations within the anoxic zone (Konovalov and Murray, 2001; Konovalov et al., 2001; Neretin et al., 2001).

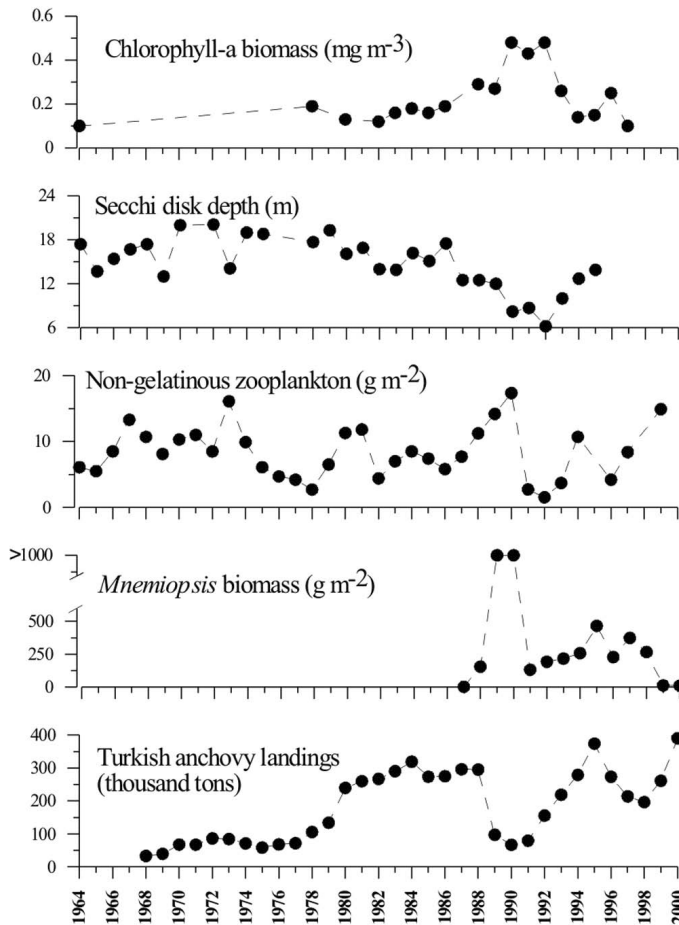


Figure 33.8 Long-term variability of (a) chlorophyll concentration (mg m^{-3}), (b) secchi disk depth (m), (c) non-gelatinous mesozooplankton biomass (g m^{-2}), (d) *Mnemiopsis* biomass (g m^{-2}), (e) Turkish anchovy landings (ktons) (from Kideys 2002). Surface chlorophyll-a—mean values (of about 1000 samples) during May-September; Secchi disk depth (to show water transparency)—annual mean (of a total 1042 measurements during February-December period) for the central Black Sea; non-gelatinous zooplankton biomass—mean values of March, May, June, July and August (collected from several stations from the open waters at approx. biweekly intervals); *Mnemiopsis* biomass data—average of summer values (except the value of 1990 belonging to April) from around a total of 700 stations. Anchovy catch (note that since the 1980s, Turkish catches comprise the bulk of anchovy in the Black Sea).

The interannual and seasonal biomass variations of phytoplankton and zooplankton communities over the last 30 years may be classified mainly into four distinct phases depending on the major top predators controlling the lower trophic food web structure. The period from the mid-1970's to 1987 was dominated by the top predator jellyfish *Aurelia aurita*. Available data show that the impact of this species was considerable on the mesozooplankton. For example, very low mesozooplankton biomass was observed during the peak levels of this species in 1978 (Fig. 33.8c) (calculated to be around 400 million tons for the entire sea; Kideys and Romanova 2001). The phytoplankton community exhibited a major bloom during the late winter-early spring season (Fig. 33.9), following the period of active nutrient accumulation in the surface waters at the end of the winter mixing season and as soon as the water column receives sufficient solar radiation. The phytoplankton bloom was first followed by a mesozooplankton bloom of comparable intensity, which reduced the phytoplankton stock to a relatively low level and then by an *Aurelia* bloom that similarly grazed down the mesozooplankton. The phytoplankton recovered and produced a weaker late spring bloom, which triggered a steady increase in *Noctiluca* biomass during the mid-summer. As the *Aurelia* population decreased in August, first the mesozooplankton and then the phytoplankton and *Aurelia* gave rise to successive blooms during September-October. These blooms were followed by a secondary *Noctiluca* bloom in November. *Aurelia* biomass exhibited two seasonal peaks of about 2–3 gC m⁻² during May and October, and attained minimum levels during the summer and winter seasons. The summer reduction in the *Aurelia* biomass seemed to be related to food competition as both *Aurelia* and small pelagic fishes (such as anchovy and horse mackerel) feed on the same trophic levels, and the abundance of small pelagic fishes was maximal during the summer period (Gucu, 2002). Bacteria and microzooplankton biomass stayed at much lower levels than the other groups, and did not show any appreciable variation throughout the year.

The years 1989–1991 constituted the second phase in which *Aurelia* blooms were almost totally replaced by those of *Mnemiopsis* (Fig. 33.8d). Following its accidental introduction into the Black Sea in ballast waters of tankers during the early 1980s, *Mnemiopsis* community quickly dominated the entire ecosystem, because it had no predators in the Black Sea. The sudden increase in the *Mnemiopsis* population caused further reduction in the biomass of the mesozooplankton community (Fig. 33.8c) as well as fish eggs and larvae during the late 1980s (Shushkina et al., 1998). This effect, together with overfishing, ultimately caused a collapse of commercial fish stocks (anchovy, sprat and horse-mackerel) during the early 1990s (Fig. 33.8e, and Rass, 1992). *Aurelia* biomass decreased below 1 gC m⁻² throughout the year during this period. *Mnemiopsis* biomass, in contrast, which was never at measurable quantities before, reached about 1.0 gC m⁻² in August 1988. During 1989, the *Mnemiopsis* maximum was about 2.0 gC m⁻² in February-March, and was followed by a decreasing trend in June-July, and later by a second peak of about 3.0 gC m⁻² during August-September. The next set of measurements, performed during late winter-early spring 1990, also recorded a strong *Mnemiopsis* peak on the order of 3.0 gC m⁻², whereas the *Aurelia* biomass remained only around 0.5 gC m⁻². *Mnemiopsis* biomass again decreased in the late spring-summer period.

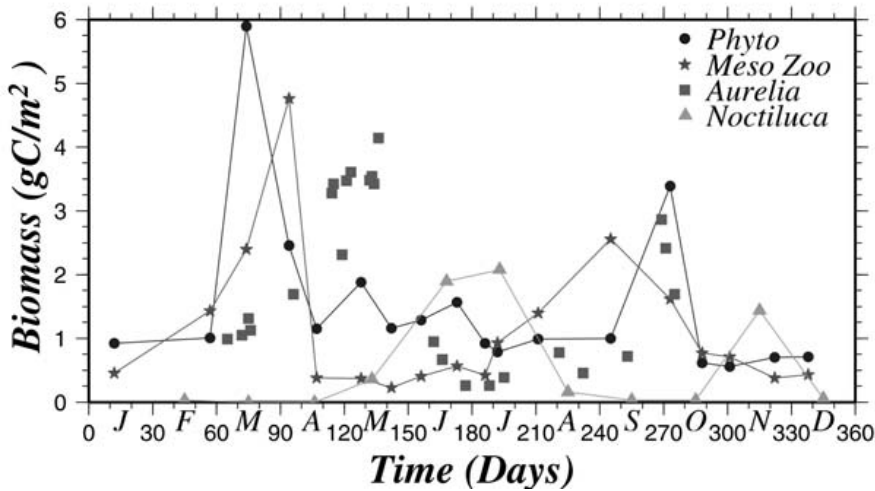


Figure 33.9 Annual distributions of total phytoplankton, mesozooplankton, *Noctiluca* and *Aurelia* biomass representing the conditions of pre-*Mnemiopsis* phase of the Black Sea ecosystem. The data for phytoplankton and mesozooplankton biomass are taken from measurements carried out at 2–4 weeks intervals during January–December 1978 at a station, off Gelendzhik along the Caucasian coast. The *Noctiluca* and *Aurelia* biomass data are taken from measurements on the Romanian shelf and the interior basin, respectively, during the late 1970s and early 1980s (from Oguz et al., 2001b).

Because the outbreak of the *Mnemiopsis* population has been limited to a relatively short period of time, its impact on all trophic levels could not be observed systematically. Measurements carried out within the interior Black Sea during February–April 1991 (Shushkina et al., 1998) indicated some shifts in timing of the phytoplankton and mesozooplankton blooms. Phytoplankton biomass showed an increasing trend starting in early January and reaching a value of $\sim 6 \text{ gC m}^{-2}$ toward the end of February. The data further indicated enhanced mesozooplankton stocks during March following the phytoplankton bloom. The surface chlorophyll-*a* data set formed by combining the Turkish, Russian, Ukrainian, Bulgarian and Romanian measurements for the period of 1990–1995 (Yilmaz et al., 1998b; Yunev et al., 2002) also exhibited peaks in winter (January–February), as well as in the spring–early summer period (May–June). Moreover, the composite data formed by measurements within the interior basin during the last decade suggested an order of magnitude decrease in *Noctiluca* biomass from the 1980's to the early 1990's (Kovalev and Piontkovski, 1998). Measurements from Sevastopol Bay during 1989 and 1990 revealed approximately a two-month shift in the *Noctiluca* biomass peaks from July to May and from November to September (Oguz et al., 2001b).

The period after 1991 represented a third stage in the ecosystem transformation in which *Mnemiopsis* stocks stabilized around 30% of their bloom level and became comparable with *Aurelia* stocks (around $\sim 1.0 \text{ gC m}^{-2}$). The main factor for reduction in the *Mnemiopsis* biomass during the 1992–1993 period, (Fig. 33.8d) was the intense winter cooling and reduction of the sea surface temperatures down to 5°C , which were unfavorable for survival of *Mnemiopsis*. After 1993, the gelatinous macrozooplankton community no longer reached a level critically competing

for food with pelagic fish groups (Kideys and Romanova, 2001). The 1993–1995 period of the ecosystem was therefore characterized by some positive sign of recovery such as an increase in fish stocks (Fig. 33.8e) and re-appearance of some zooplankton species (e.g. *Oithona nana*, *Sagitta setosa*).

The climate-induced warming during the second half of the 1990s (Fig. 33.3) caused loss or weakening of the early spring phytoplankton bloom as a result of weaker turbulent mixing and upwelling, stronger stratification and subsequently reduced upward supply of nutrients from subsurface levels. After 1995, the climate-induced bottom-up type nutrient limitation affected the entire food web. The new annual phytoplankton structure suggested by SeaWiFS chlorophyll data (Fig. 33.10) showed a major decrease of biomass during the late winter-early spring period without any major bloom signature (Oguz et al., 2003). Many higher trophic level species were characterized by reduced stocks (Fig. 33.8e).

Another peculiar feature of the ecosystem after 1995 was development of a strong early summer coccolithophore bloom over the entire basin from early-May until mid-July, contrast to their more limited abundance during the early 1980s. A comparison between the SeaWiFS and the historical coastal zone color scanner data (Cokacar et al., 2001, 2003), as well as some long-term continuous localized measurements (Moncheva and Krastev, 1997) indicates an increase in both coverage and abundance of coccolithophorids during the 1990s. The increasing contribution of coccolithophores to the early summer phytoplankton community structure during the last decade is consistent with the dramatic shifts in taxonomic composition from diatoms to coccolithophores and flagellates, as a part of transformations that took place in the Black Sea biogeochemistry and ecosystem structure under changing anthropogenic and climate forcing during the 1980s and 1990s, respectively. The climate-induced changes in the physical and biogeochemical structure of the water column (e.g. enhanced stratification and light absorption characteristics, shallower mixed layer, decreased inorganic nutrient availability) should also support wider coverage of coccolithophore blooms in the Black Sea. Finally, the period after 1998 represents a new era in which the Mediterranean species *Beroe ovata* settled in the Black Sea and started consuming *Mnemiopsis*, especially in coastal and shelf waters (Vinogradov et al., 2000; Finenko et al., 2001; Shiganova et al., 2001; Kideys, 2002). Accordingly, *Mnemiopsis* biomass started decreasing (Fig. 33.8d) at the expense of increasing mesozooplankton biomass (Fig. 33.8c) due to their reduced top-down grazing pressure on the mesozooplankton community. The top-down induced improvement in the food web may be the major cause of an increase in the pelagic fish stocks as seen in the Turkish anchovy landing data towards the end of the 1990s (Fig. 33.8e).

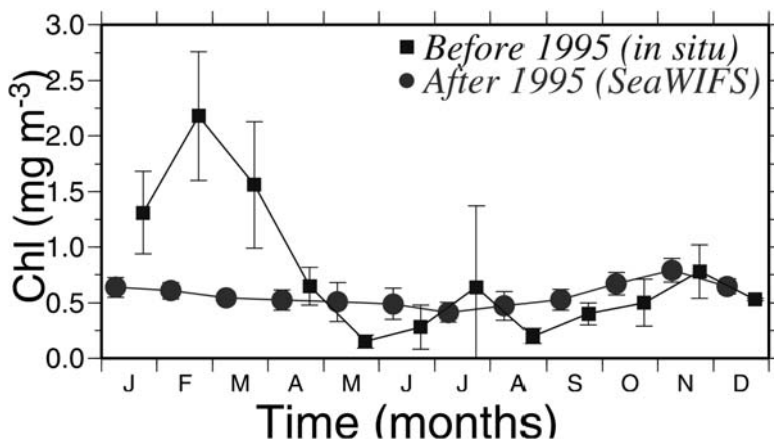


Figure 33.10 Basin-averaged, monthly-mean surface chlorophyll concentration distributions (in mg m^{-3}) before and after 1995. After 1995 distribution is obtained by averaging the OCTS and SeaWiFS ocean color data during 1997–2002 period for regions deeper than 200 m and are shown by dots. The pre-1995 data is composed from different sets of measurements carried out in deep parts of the sea and are shown by squares (from Oguz et al., 2003).

7. Interdisciplinary modeling studies

7.1. Circulation models

A series of three dimensional primitive equation-based circulation models has been used to study characteristics of the Black Sea circulation system. While earlier models had somewhat coarser horizontal and vertical resolutions, and therefore were not able to properly resolve strong horizontal and vertical density gradients as well as the narrow and steep continental slope around the periphery of the basin (e.g. Stanev, 1990), more recent models acquired eddy-resolving character by introducing more than 20 levels in the vertical and a typical grid size less than 10 km in the horizontal with respect to the baroclinic radius of deformation of greater than 20 km (e.g. Oguz et al., 1995; Besiktepe et al., 2001; Staneva et al., 2001; Beckers et al., 2002). Implementation of five different types of models having comparable complexities are particularly noted among others; the Modular Ocean Model (MOM) by Stanev (1990), Princeton Ocean Model (POM) by Oguz et al. (1995), GHER model by Stanev and Beckers (1999), Harvard Open Ocean Prediction Systems (HOPS) by Besiktepe et al. (2001), and DieCAST model by Staneva et al. (2001). MOM and HOPS have similar characteristics using z-grid on the vertical, rigid-lid, and empirical-based functional representation of the vertical eddy diffusivity and viscosity, whereas POM and GHER have bottom-following σ -coordinate, free surface, and parameterize vertical mixing by means of fairly sophisticated turbulence closure models. DieCAST also resembles MOM but has very low dissipation and forth-order accuracy. All these models explored various dynamical features of the sea concerned with water-mass formation processes, mesoscale dynamics related to eddy generation- dissipation processes and eddy-eddy, and eddy-mean flow interactions, relative contributions of different processes controlling the circulation system, coastal-open sea interactions and ex-

changes, wave characteristics, tracer distributions, forecast-related data-driven simulations, etc. They indicated that the overall basin circulation is controlled primarily by the wind stress forcing during the year, and further modulated by the seasonal evolution of the surface thermohaline fluxes, and mesoscale features arising from the basin's internal dynamics. Topography, together with the coastline configuration of the basin, is shown to exert important roles in controlling the pattern of the Rim Current system. The fresh water discharge from the Danube was also shown to generate a basin-wide buoyancy-driven circulation similar to those of the wind forcing.

Rossby waves were shown form spontaneously within the eastern basin and propagate to the west within the deep basin with a phase velocity of $\sim 3 \text{ km day}^{-1}$, and eventually dissipate within the western basin (Rachev and Stanev, 1997; Stanev and Rachev, 1999). Different modes of Rossby waves were thus considered to contribute to the number of gyres forming the interior cyclonic cell. Moreover, they were shown to induce strong changes in the depth of the pycnocline, enhance the amplitude of the Rim Current and modulate exchange between cyclonic and anticyclonic eddies located on two different sides of the Rim Current frontal zone. These exchanges are further controlled on shorter time and spatial scales by mesoscale dynamics introduced by the baroclinic-barotropic (hence mixed) instability mechanism associated with strong vertical and horizontal shears associated with the Rim Current frontal structure. On the other hand, the models (Oguz et al., 1995; Stanev and Staneva, 2000; Besiktepe et al., 2001; Staneva et al., 2001; Beckers et al., 2002) provided clear examples of meander steepening, eddy detachment and growth and splitting, and therefore further contributed to variability of the circulation. A further complexity was shown to be introduced by coastal-trapped waves propagating cyclonically around the basin (coast to the right of the propagation direction) with phase speed of about $5\text{--}8 \text{ km day}^{-1}$ (Staneva et al., 2001). The data-driven simulations by Besiktepe et al. (2001) attempted to predict a season-long transformation of the circulation during summer-autumn 1992 following initialization of the model by a particular hydrographic data set optimally interpolated to the model grid, and subsequently forwarded in time under wind stress and fresh water inflow forcings. The model identified distinct dynamical processes responsible for generation and evolution of important mesoscale circulation features in different parts of the basin. Some of the models (Oguz and Rizzoli, 1996; Stanev et al., 1997; Staneva and Stanev, 2002) were designed to explore cold intermediate water mass formation process, with particular emphasis on the relative contributions of the shelf and cyclonic interior to the formation process, and depth of convection depending on the intensity and number of cooling events as well as their interannual variability. In some studies, the circulation models were extended to study tracer distributions when coupled with appropriate tracer models. Staneva et al. (1999) used the distribution of the artificial radionuclide, ^{137}Cs , to investigate mixing and ventilation characteristics of the Black Sea surface and intermediate waters. The simulations suggested isopycnal sinking and spreading as the main mechanism of the tracer distribution. Diapycnal mixing had only secondary contribution in some particular regions during the time of CIW formation.

7.2. Food web models

Because fishery plays such an important role in the region's economy and because the biological community has been so heavily impacted over the past decades, much attention has been given to constructing food web models of the Black Sea ecosystem. The simplest approach for modeling the structure and functioning of the plankton community was to employ zero-dimensional biological models representing the vertically-averaged conditions within a prescribed surface layer, and introducing physical processes diagnostically from the available data (Lebedeva and Shushkina, 1994; Eeckhout and Lancelot, 1997; Lancelot et al., 2002b). The second approach was to utilize depth-dependent models providing finer vertical representation and physical-biogeochemical coupling through simulation of temperature and vertical diffusivity in the water column by means of a physical model (Oguz et al., 1996, 1999, 2000, 2001b; Gregoire et al., 1998, Gregoire and Lacroix, 2001). Models having an intermediate complexity in terms of their vertical resolution constituted the third approach (Oguz and Salihoglu, 2000; Oguz et al., 2001c). They involved multi-layer representation of the vertical structure, an entrainment parameterization, and coupling with a layered circulation model. They therefore provided a computationally more efficient tool particularly in three-dimensional applications. Majority of these models were applied for one-dimensional simulations (i.e. no horizontal dependence), except a few basin-wide, three-dimensional implementations (Gregoire et al., 1998; Gregoire and Lacroix, 2001; Oguz and Salihoglu, 2000).

Lebedeva and Shushkina (1994) explored ecosystem characteristics before and after the introduction of *Mnemiopsis* for the central Black Sea conditions. Their model included single groups of phytoplankton, bacteria, protozoa (i.e. microzooplankton), mesozooplankton, medusae and *Mnemiopsis* together with organic and inorganic forms of phosphate. The model was able to explain quantitatively how the shift in major gelatinous carnivore population from *Aurelia aurita* to *Mnemiopsis leidyi* resulted in changes in two isolated phytoplankton blooms taking place in autumn and early spring periods of the pre-*Mnemiopsis* phase to an extended autumn-to-winter bloom ended by a stronger early spring bloom. Their simulation of higher winter phytoplankton biomass was related to less efficient mesozooplankton grazing pressure on phytoplankton, and was found to be consistent with the observed winter bloom of 1991 within the interior part of the sea.

Eeckhout and Lancelot (1997) and Lancelot et al. (2002b) studied the role of nutrient enrichment on destabilization of the northwestern shelf ecosystem within the last three decades. Particular emphasis was given to establishing the link between changes in nutrients, phytoplankton composition and food web structures during the course of ecosystem evolution. Their ecosystem model configuration is the most sophisticated one used in the Black Sea, and incorporates carbon, nitrogen, phosphorus and silicon cycling of both planktonic and benthic systems. Phytoplankton were represented by three different groups (diatoms, flagellates, opportunistic species), microzooplankton, mesozooplankton, opportunistic herbivore *Noctiluca*, and gelatinous carnivore species *Aurelia*, *Mnemiopsis*, as well as two different biodegradability classes of particulate and dissolved organic matter. The simulations suggest that phosphorus is the major limiting nutrient for the northwestern shelf instead of nitrate or silicate. In the case of a well-balanced

N:P:Si nutrient enrichment scenario, the planktonic food web was characterized by a linear, diatom-copepod type food chain. The gelatinous carnivores were enhanced through their feeding on copepods. In the case of unbalanced nutrient inputs, such as nitrogen or phosphate deficiency, the food chain was dominated by microbial processes. Under these conditions, significant reduction in gelatinous organisms was predicted as observed in the 1990s. The major implication of the latter simulations was to relate the observed positive sign of recovery in the ecosystem to the reduction in anthropogenic nutrient supply, in particular phosphate.

According to the modeling studies by Oguz et al. (1996, 1998, 1999, 2001b), an early spring diatom bloom and a subsequent increase in mesozooplankton stocks are robust signatures of the annual plankton structure of the Black Sea ecosystem, and are seen in every data set irrespective of the type of top-down grazing control by top predators (e.g. Sorokin, 2002; Vedernikov and Demidov, 1997). The autotrophs and heterotrophs, however, have different responses during the rest of the year, depending on the nature of grazing pressure exerted by gelatinous predators. Oguz et al. (2001b) utilized a nitrogen-limited ecosystem model comprising two groups of phytoplankton (small and large fractions), microzooplankton, mesozooplankton, bacterioplankton, *Noctiluca*, *Aurelia*, *Mnemiopsis*, dissolved and particulate organic nitrogen, ammonium and nitrate compartments. They performed simulations to explore characteristic features of the *Aurelia*- and *Mnemiopsis*-dominated ecosystems similar to those studied by Lebedeva and Shushkina (1994). The *Aurelia*-dominated ecosystem model configuration was shown to quite realistically simulate the annual cycles of phytoplankton, mesozooplankton, *Noctiluca*, *Aurelia* (Fig. 33.11) consistent with the observations (Fig. 33.9). The top-down control by *Mnemiopsis* was then shown to alter the autotroph and heterotroph annual biomass structures. The annual phytoplankton structure consisted of three successive and intense bloom events during winter, spring and summer. The winter bloom may be regarded as a modified version of the late winter event seen in the pre-*Mnemiopsis* era. The other two blooms may also be interpreted as the two-month shifts in the late spring-early summer and the autumn events of the pre-*Mnemiopsis* case. The winter phytoplankton bloom was developed by a particular form of grazing pressure arising due to the specific annual *Mnemiopsis* biomass cycle. It caused an almost complete depletion of the microzooplankton, mesozooplankton and *Noctiluca* stocks towards the end of the autumn season. The lack of grazing on the phytoplankton community then promoted earlier growth starting by the beginning of January. In the previous case of *Aurelia* dominance, on the other hand, the zooplankton community developed following the autumn bloom event prevented early initiation of phytoplankton growth in winter months. The other interesting feature was the shift of *Noctiluca* peaks to two months earlier with respect to the pre-*Mnemiopsis* period, as reported by the observations.

Gregoire et al. (1988) and Gregoire and Lacroix (2001) attempted to model the three-dimensional structure of the Black Sea ecosystem using a sophisticated physical-biological model using 15 km horizontal grid resolution and 25 vertical levels. In Gregoire et al. (1988), the physical model providing three dimensional fields of currents, temperature and vertical eddy diffusivity was coupled with 13 compartment biological model representing the ecosystem by three functional groups of phytoplankton, two groups of herbivorous zooplankton, bacteria, ammonium, nitrate, phosphate, silicate, particulate and dissolved organic nitrogen

and particulate silicate. In Gregoire and Lacroix (2001), the biological model was more simplified involving single groups of phytoplankton and zooplankton as well as a simplified nitrogen cycle, but oxygen dynamics were included. The results of the model simulations reproduced major horizontal and vertical structures of physical and biochemical properties such as the seasonal cycle of phytoplankton blooms within the interior basin and more extended blooms within the northwestern shelf. A similarly simple nitrogen-based model formed by two groups of phytoplankton and zooplankton, detritus, ammonium and nitrate using a three layer representation of the upper layer water column was used to assess impact of eddy-dominated horizontal circulation on the spatial and temporal variations of plankton biomass (Oguz and Salihoglu, 2000). All these models suggested combination of wind-driven coastal upwelling, eddy-pumping, entrainment due to mixed layer deepening, and vertical diffusion controlling the nutrient supply to the euphotic zone, and generating phytoplankton blooms of both new and regenerated origin during October-December and March-May periods. Eddy-induced lateral transports and asymmetries at the mixed- and intermediate-layer depths, as well as on nutrient fluxes, support complex patterns of biomass distributions.

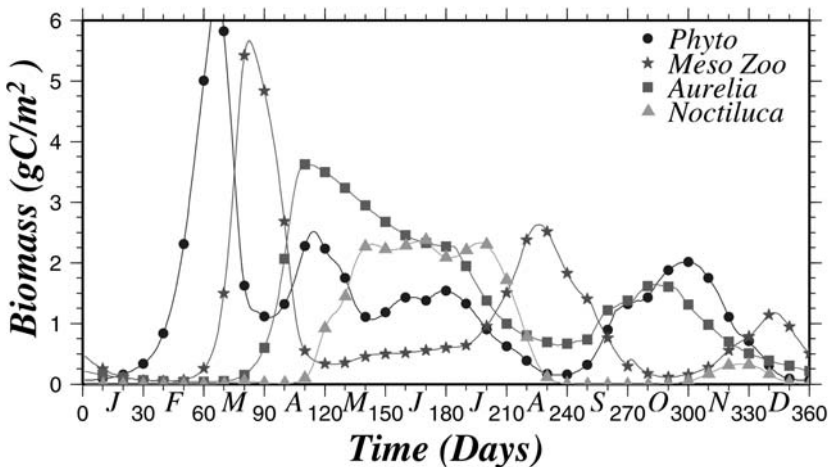


Figure 33.11 Annual distributions of total phytoplankton, mesozooplankton, *Noctiluca* and *Aurelia* biomass representing the conditions of pre-*Mnemiopsis* phase of the Black Sea ecosystem simulated by the model described by Oguz et al. (2001b).

7.3. Redox cycling models

Because of the relatively broad and stable character of the suboxic-anoxic transition zone, the Black Sea is an ideal site to model redox processes. The nitrogen and sulfur cycles were first modeled by Yakushev and Neretin (1997) constraining sulfide oxidation by oxygen alone. Sulfur cycling involved abiogenic oxidation to thiosulfate followed by its bacterial oxidation to sulfate by thiobasili. Because this bacterium requires oxygen, sulfur oxidation depends on the availability of oxygen. The lowest oxygen concentration requirement for oxidation was set to 2 μM , and its maximum efficiency was assumed to take place at oxygen concentrations

greater than $9 \mu\text{M}$. The Yakushev and Neretin model thus requires a continuous supply of oxygen to drive the sulfur cycle. This supply was provided by a downward diffusive oxygen flux using a vertical eddy diffusivity of $1 \times 10^{-5} \text{ m}^2 \text{ s}^{-1}$, which appears to be an order of magnitude higher than those estimated from microstructure measurements and hydrographic data for such strongly stratified conditions (Gregg and Ozsoy, 1999). Their simulations therefore show overlapping dissolved oxygen and sulfide concentrations. In Yakushev (1998) and Debolskaya and Yakushev (2002), this model was extended to incorporate simplified manganese cycling in which particulate manganese used for oxidizing hydrogen sulfide was produced by oxidation of dissolved manganese with oxygen as the data seem to indicate. A similar model based on the same concept of sulfide-oxygen interaction was given by Belyaev et al. (1997). This model was developed specifically for the northwestern shelf ecosystem, and a case study of its implementation was described by Lyubartseva and Lyubartsev (1998).

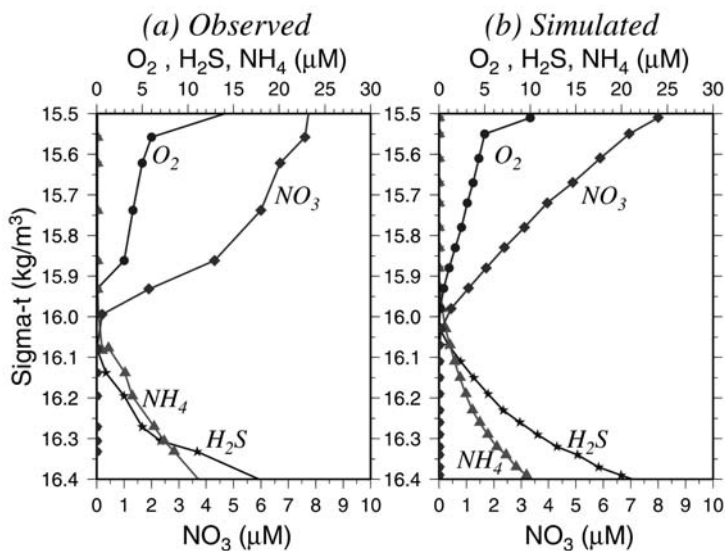


Figure 33.12 (a) Observed, and (b) simulated profiles of dissolved oxygen, hydrogen sulphide, nitrate and ammonium within the Suboxic Layer and onset of the sulfide zone (from Oguz et al., 2002b).

Oguz et al. (2001a) proposed a model with a somewhat different set of redox reactions catalyzed by the manganese cycle. The model was based on the hypothesis that the anaerobic sulfide oxidation and nitrogen transformations were the primary mechanisms controlling the interface structure between the suboxic and anoxic layers. Following Murray et al. (1995, 1999), it was proposed that the upward fluxes of sulfide and ammonium are oxidized by Mn(III, IV) and Fe(III) species, whereas the downward flux of nitrate may be reduced by dissolved manganese and ammonium. Mn(II) oxidation and Mn(IV) reduction are both microbially catalyzed (Tebo, 1991; Francis and Tebo, 1999), but dissolved abiotic, chemical reduction is also thought to play a role in Mn(IV) reduction by sulfide (e.g. Mil-

lero, 1991). In Oguz et al. (2001a), only manganese cycling was included and the additional contribution of iron cycling was neglected for simplicity. The anammox reaction, whose importance in the Black Sea was recently shown by Kuypers et al. (2003), was also not included. Dissolved manganese oxidized by nitrate was found to be responsible for the production and cycling of particulate manganese, which in turn oxidized hydrogen sulfide and ammonium transported upwards from deeper levels. Even with such a highly simplified representation of the redox processes, the model provided a realistic suboxic-anoxic interface zone structure, and was able to give quantitative evidence for the presence of an oxygen depleted and non-sulfidic suboxic zone (Fig. 33.12). This model pointed out the crucial role of the downward supply of nitrate from the overlying nitracline zone and for the upward transport of dissolved manganese from the anoxic pool below for maintenance of the suboxic layer.

The food web and the suboxic-anoxic interface redox cycle models provided by Oguz et al. (2001a,b) were then coupled with each other as well as a water column oxygen cycling model in order to provide a model capable of providing a unified description of the dynamically coupled oxic-suboxic-anoxic system (Oguz et al., 2000). The combined model (Fig. 33.13) was comprised of a nitrogen-based pelagic plankton system coupled through particulate and dissolved organic matter fluxes to the water column nitrogen cycle model including transformations among ammonium, nitrite and nitrate. This system was then coupled with a model of oxygen and redox dynamics describing oxygen variations within the euphotic zone, oxycline and near the suboxic-anoxic interface zone. These processes were finally linked to manganese and sulfur transformations. The model further allowed on-line coupling with the physical model providing vertical eddy diffusivity and temperature data to the biological model. The physical model, which was documented by Oguz et al. (1996), was based on the Princeton Ocean Model in which wind- and buoyancy-induced vertical mixing were parameterized by a level 2.5 turbulence closure model. The simulations indicated that oxygen consumption during remineralization and nitrification, together with the lack of ventilation of subsurface waters due to the presence of strong vertical stratification, are two main factors limiting aerobic biogeochemical activity to the upper 75 m of the water column, which approximately corresponds to the level of nitrate maximum. The position of the upper boundary and thus the thickness of the suboxic layer are controlled by upper layer biological processes. The quasi-permanent character of this layer and the stability of the suboxic-anoxic interface within the last several decades are maintained by a constant rate of nitrate supply from the nitrate maximum zone.

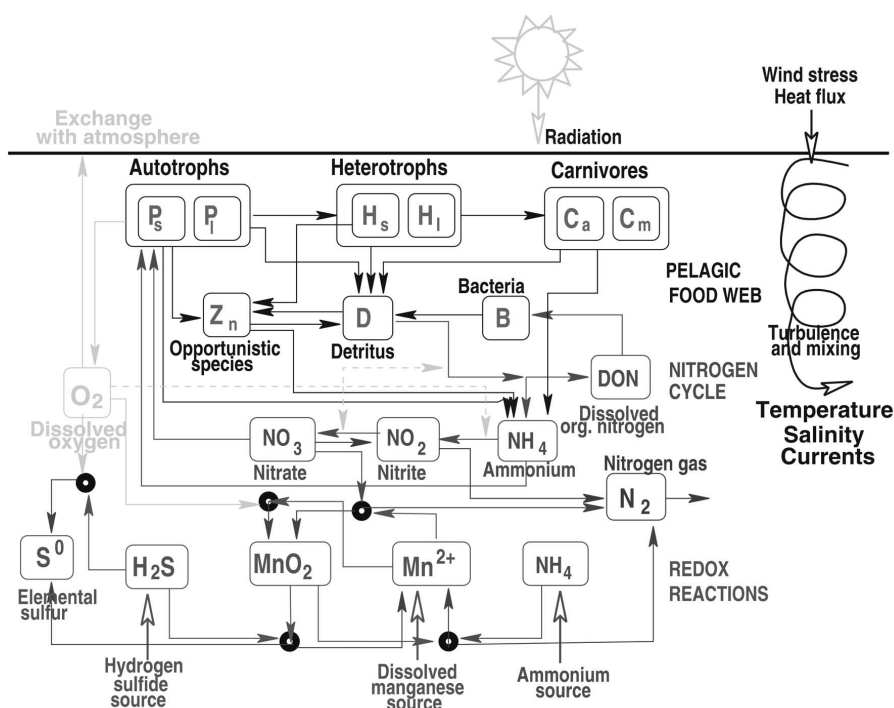


Figure 33.13 Schematic representation of the major processes and interactions between biogeochemical model compartments. P_s , P_l denote large and small phytoplankton groups, H_s is microzooplankton, H_l is mesozooplankton, C_a is jellyfish *Aurelia aurita*, C_m is ctenophore *Mnemiopsis leidyi*, Z_n is opportunistic dinoflagellate *Noctiluca scintillans*, MnO_2 is particulate manganese. Meaning of the other variables are as shown in the figure. The biogeochemical model is coupled to the physical model through vertical diffusivity and temperature (from Oguz et al., 2002b).

8. Conclusions

Implementation of various contemporary ocean research programs in the last decade have generated considerable progress toward understanding the Black Sea's basic physical and biogeochemical processes. A series of basin-wide, quasi-synoptic, multi-ship research cruises were accomplished, and complemented by analysis of satellite data and interdisciplinary modeling studies. Physical and biogeochemical data accumulated from these studies were able to resolve many features of the Black Sea circulation and ecosystem structure. The description and understanding of basin scale dynamical features has reached maturity. Modelling and data assimilation tools have been developed, and implemented but they still require further calibration and validation exercises by availability of new data sets. These efforts also led to substantial improvement in our understanding of biogenic element cycling, pelagic and benthic ecosystems carbon and energy flows, various distinct biogeochemical processes taking place across the anoxic interface, as well as their coupling to the circulation, and horizontal/vertical transport mechanisms. Knowledge and modeling of the coastal and shelf areas are still scarce and await

implementation of a systematic observation and modeling program. More comprehensive future studies on the climate-driven ecosystem changes are expected to provide insights for sustainable use of marine living resources in the Black Sea, and effective management policies. More elaborate deterministic models will be particularly useful for the mechanistic understanding of the ecosystem as a whole, testing various hypotheses put forward for explaining observed features, assessing relative contributions of different mechanisms, predicting optimal near-real time estimates of large scale flow and biogeochemical fields and forecasting future state of the ecosystem.

Bibliography

- Afanasyev, Y.D., A.G. Kostianoy, A.G. Zatsepin, and P.M. Poulain, 2002. Analysis of velocity field in the eastern Black Sea from satellite data during the Black Sea '99 experiment. *J. Geophys. Res.*, **107**, 10.1029/2000JC000578.
- Aksu, A.E., R.N. Hiscott, and D. Yasar, 1999. Oscillating Quarternary water levels of the Marmara Sea and vigorous outflow into the Aegean Sea from the Marmara Sea-Black Sea drainage corridor. *Marine Geology*, **153**, 275–302.
- Aksu, A.E., R.N. Hiscott, M.A. Kaminsky, P.J. Mudie, H. Gillespie, T. Abrajano, and D. Yasar, 2002. Last glacial-Halocene paleoceanography of the Black Sea and Marmara Sea: Stable isotopic, foraminiferal, and coccolith evidenced. *Marine Geology*.
- Almazov, N. M., 1961. Stok ratverennykh soley I bogennykh veschetv kotorye vynoseatsya rekami USSR v Chernoe More. *Naukovi Zapiski Odes. Biol. St. Kiev* 3, pp. 99–107.
- Ballard, R.D., D.F. Coleman, G.D. Rosenberg, 2000. Further evidence of abrupt Holocene drowning of the Black Sea shelf. *Mar. Geol.*, **170**, 253–261.
- Basturk, O., C. Saydam, I. Salihoglu, L. V. Eremeeva, S. K. Konovalov, A. Stoyanov, A. Dimitrov, A. Cociasu, L. Dorogan, and M. Altabet, 1994. Vertical variations in the principle chemical properties of the Black Sea in the autumn of 1991. *J. Marine Chemistry*, **45**, 149–165.
- Basturk, O., S.Tugrul, S.Konovalov, I., Salihoglu, 1998a. Effects of circulation on the saptial distributions of principle chemical properties and unexpected short- and long-term changes in the Black Sea. In: *Ecosystem modeling as a management tool for the Black Sea*. Ivanov, L.I. and T. Oguz (eds.), NATO ASI Series, Vol. 47, Kluwer Academic publishers, Netherlands, pp. 39–54.
- Basturk, O., I. I. Volkov, S. Gokmen, H. Gungor, A.S Romanov, and E.V. Yakushev, 1998b. International expedition on board R.V. Bilim in July 1997 in the Black Sea. *Oceanology (English trans.)*, **38**, 429–432.
- Beckers, J.M., M.L. Gregoire, J.C.J. Nihoul, E. Stanev, J. Staneva and C. Lancelot, 2002. Hydrodynamical processes governing exchanges between the Danube, the North-Western continental shelf and the Black Sea's basin simulated by 3D and box models. *Estuarine, Coastal and Shelf Science*, **54**, 453–472.
- Belyaev, V. I. , E.E. Sovga, and S.P. Lyubartseva, 1997. Modelling the hydrogen sulfide zone of the Black Sea. *Ecological Modelling*, **13**, 51–59.
- Besiktepe, S.T., C.J., Lozano, and A.R., Robinson, 2001. On the summer mesoscale variability of the Black Sea. *J. Mar. Res.*, **59**, 475–515.
- Brewer, P.G. and D.W. Spencer, 1974. Distribution of some trace elements in the Black Sea and their flux between dissolved and particulate phases. In: *The Black Sea- Geology, Chemistry, and Biology*. E.T. Degens and D.A. Ross, eds. The American Association of Petroleum Geologists, Memoir 20, pp. 137–143.
- Buesseler, K.O., H.D. Livingston, L.Ivanov, and A. Romanov, 1994. Stability of the oxic-anoxic interface in the Black Sea. *Deep-Sea Res. I*, **41**, 283–296.

- Burlakova, Z.P., L.V., Ereemeeva, and S.K. Konovalov, 1997. Particulate organic matter of Black Sea euphotic zone. In: *Sensitivity to change: Black Sea, Baltic Sea and North Sea*, Özsoy, E. and A. Mikaelyan. (eds.), NATO ASI Series, Environment-Vol. 27, Kluwer Academic publishers, Netherlands, pp. 223–238.
- Cagatay, M.N., 1999. Geochemistry of the late Pleistocene-Holocene sediments of the Black Sea basin. In: *Environmental degradation of the Black Sea: Challenges and Remedies*. S. Besiktepe, U. Unluata and A. Bologa, (eds). NATO-ASI Series, Environmental Security, Vol. 56, Kluwer Academic Publishers, Dordrecht, pp. 9–22.
- Cagatay, M.N, N. Gorur, A. Algan, C.J. Eastoe, A. Tchapylyga, D. Ongan, T. Kuhn, I. Kuscu, 2000. Late Glacial-Holocene paleoceanography of the Sea of Marmara: timing of connections with the Mediterranean and the Black Seas. *Mar. Geol.* **167**, 191–206.
- Calvert, S.E. and Fontugne, 1987. Stable carbon isotopic evidence for the marine origin of the organic matter in the Holocene Black Sea sapropel. *Chemical Geology (Isotope Geoscience Section)*, **66**, 315–322.
- Charlson, R. J., J. E. Lovelock, M. O. Andreae and S. G. Warren, 1987. Oceanic phytoplankton, atmospheric sulphur, cloud albedo and climate: A geophysiological feedback, *Nature*, **326**, 655–661.
- Charlson, R. J., J. Longner, H. Rodhe, C. B. Leavy, and S. G. Warren., 1991. Perturbation of the Northern hemisphere radiative balance by backscattering from anthropogenic sulphate aerosols, *Tellus*, **43A**, 152–163.
- Coban-Yldz, Y., G., Chiavari, D., Fabbri, A.F., Gaines, G., Galetti, S.Tugrul, 2000a. The abundance and elemental composition of Black Sea seston: confirmation by pyrolysis-GC/MS. *Marine Chemistry*, **69**, 55–67.
- Coban-Yldz, Y., S., Tugrul, D., Ediger, A., Ylmaz, S.C. Polat, 2000b. A comparative study on the abundance and elemental composition of POM in three interconnected basins: the Black, the Marmara and the Mediterranean Seas. *Mediterranean Marine Science*, **1**, 51–63.
- Coban-Yldz Y., M.A, Altabet, A., Ylmaz, S. Tugrul and I. Salihoglu, 2003. Carbon and nitrogen isotopic ratios of suspended particulate organic matter in the Black Sea water column. *Deep-Sea Research*, submitted manuscript.
- Cociasu, A., L. Dorogan, C. Humborg and L. Popa, 1996. Long-term ecological changes in the Romanian coastal waters of the Black Sea. *Marine Pollution Bulletin*, **32**, 32–38.
- Codispoti, L.A., G.E. Friederich, J.W. Murray, and C.M. Sakamoto, 1991. Chemical variability in the Black Sea: implications of continuous vertical profiles that penetrated the oxic/anoxic interface. *Deep-Sea Res. I*, **38**, Suppl.2, S691-S710.
- Cokacar, T., N. Kubilay, and T. Oguz, 2001. Structure of *Emiliania huxleyi* blooms in the Black Sea surface waters as detected by SeaWiFS imagery. *Geophys. Res. Letters*, **28(24)**, 4607–4610.
- Cokacar, T., T. Oguz, and N. Kubilay, 2004. Interannual variability of the early summer coccolithophore blooms in the Black Sea: impacts of anthropogenic and climatic factors. To appear in *Deep-Sea Res. I*, **51**, 1017–1031
- Debolskaya, E.I., and E.V. Yakushev, 2002. The role of suspended manganese in hydrogen sulfide oxidation in the Black Sea redox-zone. *Water Resources*, **29**, 72–77.
- Di Iorio, D. and H. Yuce, 1998. Observations of Mediterranean flow into the Black Sea. *J. Geophys. Res.*, **104**, 3091–3108.
- Duce, R.A., Liss, P.S., Merrill, J.T., Atlas, E.L., Buat-Menart, P., Hicks, B.B., Miller, J.M., Prospero, J.M., Arimoto, R., Church, T.M., Ellis, W., Galloway, J.N., Hansen, L., Jickells, T.D., Knap, A.H., Reinhardt, K.H., Schneider, B., Soudine, A., Tokos, J.J., Tsunogai, S., Wollast, R. and Zhou, M., 1991. The atmospheric input of trace species to the world ocean, *Global Biogeochem. Cycles*, **5**, 193–259.
- Eeckhout, D.V. and C. Lancelot, 1997. Modeling the functioning of the northwestern Black sea ecosystem from 1960 to present. In: *Sensitivity to change: Black Sea, Baltic Sea and North Sea*, NATO Sci. Partnership Sub-series 2, vol. 27, E. Ozsoy and A. Mikaelyan, eds. Kluwer Acad., Norwell, Mass., pp. 455–468.

- Eremeev, V.N., 1996. Hydrochemistry and dynamics of the hydrogen-sulfide zone in the Black Sea. *Unesco Reports in Marine Science*, R.C. Griffiths, eds. Unesco 1996, 114 pp.
- Faschuk, D.Ya., T.A. Ayzatullin, V.V. Dronov, T.M. Pankratova, and M.S. Finkelshteyn, 1990. Hydrochemical structure of the layer of co-existence of oxygen and hydrogen sulfide in the Black Sea and a possible mechanism of its generation. *Oceanology (English transl.)*, **30**, 185–192.
- Finenko, G.A., Z.A. Romanova, G.I. Abolmasova, B.E. Anninsky, L.S. Svetlichny, E.S. Hubareva, L. Bat, and A.E. Kdeys, 2003. Ingestion, growth and reproduction rates of the alien *Beroe ovata* and its impact on the plankton community in the Black Sea. *J. Plankton Res.*, **25**, 539–549.
- Francis, C.A. and B.M. Tebo, 1999. Marine bacillus spores as catalyst for oxidative precipitation and sorption of metals. *J. Mol. Microbiol. Biotechnol.*, **1**, 71–78.
- Fry, B., H.W., Jannasch, S.J., Molyneaux, C.O., Wirsén, J.A. Muramoto, and S., King, 1991. Stable isotope studies of the carbon, nitrogen and sulfur cycles in the Black Sea and the Cariaco Trench. *Deep-Sea Res.*, **38**, S1003-S1019.
- Garnier, J., G. Billen, E. Hannon, S. Fonbonne, Y. Vdenina and M. Soulie, 2002. Modeling transfer and retention of nutrients in drainage network of the Danube River. *Estuarine, Coastal and Shelf Science*, **54**, 285–308.
- Gawarkiewicz, G., G. Korotaev, S. Stanichny, L. Repetin, and D. Soloviev, 1999. Synoptic upwelling and cross-shelf transport processes along the Crimean coast of the Black Sea. *Cont. Shelf Res.*, **19**, 977–1005.
- Ginsburg, A.I., A.G., Kostianoy, D.M., Soloviev, S.V., Stanichny, 2000. Remotely sensed coastal/deep-basin water exchange processes in the Black Sea surface layer. In *Satellites, Oceanography and Society*, D. Halperned. Elsevier Oceanography Series, Amsterdam, 63, pp. 273–285.
- Ginsburg, A.I., A.G., Kostianoy, N.P., Nezlin, D.M., Soloviev, S.V., Stanichny, 2002a. Anticyclonic eddies in the northwestern Black Sea. *J. Mar. Syst.*, **32**, 91–106.
- Ginsburg, A.I., A.G., Kostianoy, V.G., Krivosheya, N.P., Nezlin, D.M., Soloviev, S.V., Stanichny, V.G. Yakubenko, 2002b. Mesoscale eddies and related processes in the northeastern Black Sea. *J. Mar. Syst.*, **32**, 71–90.
- Gorur, N., M.N. Cagatay, O. Emre, B. Alpar, M. Sakinc, Y. Islamoglu, O. Algan, T. Erkal, M. Kecer, R. Akkok, G. Karlik, 2001. Is the abrupt drowning of the Black Sea shelf at 7150 yr BP a myth? *Mar. Geol.*, **176**, 65–73.
- Grashoff, K., 1975. The hydrochemistry of landlocked basins and fjords. In: *Chemical Oceanography*, J.P. Riley and C. Skirrow, eds, Academic Press, New York, pp. 456–497.
- Gregg, M.C. and E. Ozsoy, 1999. Mixing on the Black Sea shelf north of the Bosphorus. *Geophys. Res. Letters*, **26**, 1869–1872.
- Gregoire, M., J.M. Beckers, J.C.J. Nihoul and E. Stanev, 1998. Reconnaissance of the main Black Sea's ecohydrodynamics by means of a 3D interdisciplinary model. *J. Mar. Syst.*, **16**, 85–106.
- Gregoire, M., and G. Lacroix, 2001. Study of oxygen budget of the Black Sea waters using a 3D coupled hydrodynamical-biochemical model. *J. Mar. Syst.*, **31**, 175–202.
- Gücü, A.C., 2002. Can overfishing be responsible for the successful development of *Mnemiopsis*? *Estuarine, Coastal and Shelf Science*, **54**, 439–451.
- Hay, B.J., 1994. Sediment and water discharge rates of Turkish Black Sea rivers before and after hydropower dam constructions. *Environmental Geology*, **23**, 276–283.
- Humborg, C., V. Ittekkot, A. Cociasu, and B. Bodungen, 1997. Effect of Danube River dam on Black Sea biogeochemistry and ecosystem structure. *Nature*, **386**, 385–388.
- Ivanov, L.I. and A.S. Samodurov, 2001. The role of lateral fluxes in ventilation of the Black Sea. *J. Mar. Syst.*, **31**, 159–174.
- Jannasch, H.W., C.O. Wirsén, and S.J. Molyneaux, 1991. Chemoautotrophic sulfur-oxidizing bacteria from the Black Sea. *Deep-Sea Res.*, **38**, Suppl.2A, S1105-S1120.

- Jorgensen, B.B., H. Fossing, C.O. Wirsen, and H.W. Jannasch, 1991. Sulfide oxidation in the anoxic Black Sea chemocline. *Deep-Sea Res.*, **38**, Suppl.2A, S1083-S1104.
- Kaminski, M.A.; A. Aksu, M. Box, R.N. Hiscott, S. Filipescu, M. Al-Salameen, 2002. Late Galacialto Holocene benthic foraminifera in the Sea of Marmara: implications for Black Sea-Mediterranean Sea connections following the last deglaciation. *Mar. Geol.*, **190**, 165–202.
- Karl, D.M., and G.A. Knauer, 1991. Microbial production and particle flux in the upper 350 m of the Black Sea. *Deep Sea Res.*, **38**, Supp. 2A, S655-S661.
- Kempe, S., A.R. Diercks, G. Liebezeit, and A. Prange, 1991. Geochemical and structural aspects of the pycnocline in the Black Sea (R/V Knorr 134–8 Leg 1, 1988). In: *Black Sea Oceanography*, NATO ASI Series C-Vol.351, E.Izdar and J.W. Murray, eds, Kluwer Academic Publishers, pp. 89–110.
- Kideys, A.E., 2002. Fall and rise of the Black Sea ecosystem, *Science*, **297**, 1482–1484.
- Kideys, E.A., and Z.A. Romanova, 2001. Distribution of gelatinous macrozooplankton in the southern Black Sea during 1996–1999, *Mar. Biol.*, **139**, 535–547.
- Kodina, L.A., M.P., Bogacheva, S.V., Lyutsarev, 1996. Particulate organic carbon in the Black Sea: Isotopic composition and origin. *Geochemistry International*, **9**, 884–890.
- Konovalov, S.K., and J.W. Murray, 2001. Variations in the chemistry of the Black Sea on a time scale of decades (1960–1995). *J. Mar. Syst.*, **31**, 217–243.
- Konovalov, S.K., L.I. Ivanov, and A.S. Samodurov, 2001. Fluxes and budget of sulfide and ammonia in the Black Sea anoxic layer. *J. Mar. Syst.*, **31**, 203–216.
- Konovalov, S.K., G.W. Luther, III, G.E. Friederich, D.B. Nuzzio, B.M. Tebo, J.W. Murray, T. Oguz, B. Glazer, R.E. Trouwborst, B. Clement, K. W. Murray, A. S. Romanov, 2003. Lateral injection of oxygen with the Bosphorus plume-fingers of oxidizing potential in the Black Sea. *Limnol. Oceanogr.*, **48**, 2369–2376.
- Korotaev, G.K., O.A., Saenko, C.J., Koblinsky, 2001. Satellite altimetry observations of the Black Sea level. *J. Geophys. Res.*, **106**, 917–933.
- Korotaev, G.K., T. Oguz, A. Nikiforov, C. J. Koblinsky, 2003. Seasonal, interannual and mesoscale variability of the Black Sea upper layer circulation derived from altimeter data. *J. Geophys. Res.*, **108(C4)**, 3122, doi:10.1029/2002JC001508.
- Kovalev, A.V. and S.A. Piontkovski, 1998. Interannual changes in the biomass of the Black Sea gelatinous zooplankton. *J. Plankton Res.*, **20**, 1377–1385.
- Kovalev, A.V., U., Neirman, V.V., Melnikov, V., Belokopytov, Z., Uysal, A.E., Kideys, M., Unsal, and D., Altukov, 1998. Long term changes in the Black Sea zooplankton: the role of natural and anthropogenic factors. In: *Ecosystem Modeling as a Management Tool for the Black Sea*. L. Ivanov and T. Oguz, eds. NATO ASI Series 2, Environment-Vol.47, Kluwer Academic Publishers, Vol. 1, pp. 221–234.
- Krivosheya, V.G., V. B. Titov, I.M. Ovchinnikov, R.D. Kosyan, A.Yu. Skirta, 2000. The influence of circulation and eddies on the depth of the upper boundary of the hydrogen sulfide zone and ventilation of aerobic waters in the Black Sea. *Oceanology (Eng. Transl.)*, **40**, 767–776.
- Krivosheya, V.G., I.M. Ovchinnikov, and A. Yu. Skirta, 2002. Interannual variability of the cold intermediate layer renewal in the Black Sea. In: *Multidisciplinary investigations of the northeast part of the Black Sea*, A.G. Zatsepin and M.V. Flint, eds, Moscow, Nauka, pp. 27–39.
- Kubilyay, N. and A.C., Saydam, 1995. Trace elements in atmospheric particulates over the Eastern Mediterranean; concentrations, sources, and temporal variability. *Atmospheric Environment*, **29**, 2289–2300.
- Kubilyay, N., S. Nickovic, C. Moulin and F. Dulac (2000) An illustration of the transport and deposition of mineral dust onto the eastern Mediterranean. *Atmospheric Environment*, **34**, 1293–1303
- Kubilyay, N., M. Kocak, T. Cokacar, T. Oguz, G. Kouvarakis, N. Mihalopoulos, 2002. The Influence of Black Sea and Local Biogenic Activity on the Seasonal Variation of Aerosol Sulfur Species in the Eastern Mediterranean Atmosphere. *Global Biogeochem. Cycles*, **16(4)**, 1079, doi:10.1029/2002GB001880.

- Kuypers, M.M.M., A.O. Sliemers, G. Lavik, M. Schmid, B.B. Jorgensen, J.G. Kuenen, D.J.S. Sinninghe, M. Strous, and M.S.M. Jetten, 2003. Anaerobic ammonium oxidation by anammox bacteria in the Black Sea. *Nature*, **422**, 608–611.
- Lancelot, C., J. M. Martin, N. Panin, and Y. Zaitsev, 2002a. The North-western Black Sea: A pilot site to understand the complex interaction between human activities and the coastal environment. *Estuarine, Coastal and Shelf Science*, **54**, 279–283.
- Lancelot, C., J. Staneva, D. Van Eeckhout, J. M. Beckers, and E. Stanev, 2002b. Modeling the impact of the human forcing on the ecological functioning of the northwestern Black Sea. *Estuarine, Coastal and Shelf Science*, **54**, 473–500.
- Latif, M.A., E. Ozsoy, T. Oguz, and U. Unluata, 1991. Observation of the Mediterranean inflow into the Black Sea. *Deep-Sea Research*, **38**, Supl.2A, S711-S733.
- Lebedeva, L.P. and S. V. Vostokov, 1984. Studies of detritus formation processes in the Black Sea. *Oceanology (Engl. Transl.)*, **24(2)**, 258–263.
- Lebedeva, L.P. and E.A. Shushkina, 1994. Modelling the effect of *Mnemiopsis* on the Black Sea plankton community. *Oceanology (English transl.)*, **34**, 72–80.
- Lee, B-S., J.L. Bullister, J.W. Murray, and R.E. Sonnrup, 2002. Anthropogenic chlorofluorocarbons in the Black Sea and the Sea of Marmara. *Deep-Sea Res. I*, **49**, 895–913.
- Lewis, B.L. and W.M. Landing, 1991. The biogeochemistry of manganese and iron in the Black Sea. *Deep-Sea Res.*, **38**, Supl.2A, S773-S804.
- Lyubartseva, S.P. and V. G. Lyubartsev, 1988. Modeling of the Black Sea anoxic zone processes. In: *Ecosystem Modeling as a Management Tool for the Black Sea*. L. Ivanov and T. Oguz, eds. NATO ASI Series, 2-Environmental Security-47, Kluwer Academic Publishers, Vol. 2, pp. 385–396.
- Mikaelyan, A. S., 1997. Long-term variability of phytoplankton communities in open Black Sea in relation to environmental changes. In: *Sensitivity to change: Black Sea, Baltic Sea and North Sea*, NATO Sci. Partnership Sub-series 2, vol. 27, E. Ozsoy and A. Mikaelyan, eds., Kluwer Acad., Norwell, Mass., pp. 105–116.
- Millero, F.J., 1991. The oxidation of H₂S in Black Sea waters. *Deep-Sea Research*, **38**, Supl.2A, S1139-S1150.
- Moncheva, S., A., Krastev, 1997. Some aspects of phytoplankton long-term alterations off Bulgarian Black Sea Shelf. In: *Sensitivity to Change: Black Sea, Baltic Sea and North Sea*, E. Ozsoy, A. Mikaelyan, eds. NATO ASI Series, Vol. 27. Kluwer Academic Publishers, Dordrecht, pp. 79–94.
- Murray, J.W., H. W. Jannash, S. Honjo, R. F. Anderson, W.S. Reeburgh, Z. Top, G.E. Friederich, L.A. Codispoti, and E. Izdar, 1989. Unexpected changes in the oxic/anoxic interface in the Black Sea. *Nature*, **338**, 411–413.
- Murray, J. W., Z. Top, and E. Ozsoy, 1991. Hydrographic properties and ventilation of the Black Sea. *Deep-Sea Res.*, **38**, Supl.2A, S663–690.
- Murray, J.W., L.A. Codispoti, and G.E. Friederich, 1995. Oxidation-reduction environments: The suboxic zone in the Black Sea. In: *Aquatic chemistry: Interfacial and interspecies processes*. C.P. Huang, C.R.O'Melia, and J.J. Morgan, eds. ACS Advances in Chemistry Series No.224. pp. 157–176.
- Murray, J.W., B-S Lee, J. Bullister, and G. W. Luther III, 1999. The suboxic zone of the Black Sea. In: *Environmental Degradation of the Black Sea: Challenges and Remedies*. S. Besiktepe, U. Unluata and A. Bologna, eds. NATO ASI Series 2., 75–92.
- Neretin, L.V., I.I. Volkov, M.E. Bottcher, V.A. Grinenko, 2001. A sulfur budget for the Black Sea anoxic zone. *Deep-Sea Res. I*, **48**, 2569–2593.
- Nezlin, N.P., 2001. Unusual phytoplankton bloom in the Black Sea during 1998–1999: Analysis of remotely-sensed data, *Oceanology, (English transl.)*, **41**, 375–380.
- Oguz, T., 2002. Role of physical processes controlling oxycline and suboxic layer structure in the Black Sea, *Global Biogeochem. Cycles*, **16**, 10.1029/2001GB001465.
- Oguz, T. and L. Rozman, 1991. Characteristics of the Mediterranean underflow in the southwestern Black Sea continental shelf/slope region. *Oceanology Acta*, **14(5)**, 433.444.

- Oguz, T. and P. Malanotte-Rizzoli, 1996. Seasonal variability of wind and thermohaline driven circulation in the Black Sea: Modeling studies. *J. Geophysical Research*, **101**, 16551–16569.
- Oguz, T., S., Besiktepe, 1999. Observations on the Rim Current structure, CIW formation and transport in the western Black Sea. *Deep Sea Res. I*, **46**, 1733–1753.
- Oguz, T. and B. Salihoglu, 2000. Simulation of eddy-driven phytoplankton production in the Black Sea. *Geophys. Res. Letters*, **27**, 2125–2128.
- Oguz, T., E. Ozsoy, M.A. Latif, H.I. Sur and U. Unluata, 1990a. Modeling of hydrographically controlled exchange flow in the Bosphorus Strait. *J. Phys. Oceanogr.*, **20**, 945–965.
- Oguz, T., M.A. Latif, H. I. Sur, E. Ozsoy, and U. Unluata, 1990b. On the dynamics of the southern Black Sea. In: *The Black Sea Oceanography*, J. Murry and E. Izdar, eds, NATO/ASI Series, Kluwer Academic Publishers, Dordrecht, pp. 43–64.
- Oguz, T., P., La Violette, U., Unluata, 1992. Upper layer circulation of the southern Black Sea: Its variability as inferred from hydrographic and satellite observations. *J. Geophys. Res.*, **97**, 12569–12584.
- Oguz, T., V.S., Latun, M.A., Latif, V.V., Vladimirov, H.I., Sur, A.A., Makarov, E., Ozsoy, B.B., Kotovshchikov, V.V., Ereemeev, U., Unluata, 1993. Circulation in the surface and intermediate layers of the Black Sea. *Deep Sea Res. I*, **40**, 1597–1612.
- Oguz, T., D.G., Aubrey, V.S., Latun, E., Demirov, L., Koveshnikov, H.I., Sur, V., Diacanu, S., Besiktepe, M., Duman, R., Limeburner, V.V., Ereemeev, 1994. Mesoscale circulation and thermohaline structure of the Black sea observed during HydroBlack'91. *Deep Sea Research I*, **41**, 603–628.
- Oguz, T., P., Malanotte-Rizzoli, D., Aubrey, 1995. Wind and thermohaline circulation of the Black Sea driven by yearly mean climatological forcing. *J. Geophys. Res.*, **100**, 6846–6865.
- Oguz, T., H. Ducklow, P. Malanotte-Rizzoli, S. Tugrul, N. Nezlin, and U. Unluata, 1996. Simulation of annual plankton productivity cycle in the Black Sea by a one-dimensional physical-biological model. *J. Geophys. Res.*, **101**, 16585–16599.
- Oguz, T., L.I. Ivanov, S. Besiktepe, 1998. Circulation and hydrographic characteristics of the Black Sea during July 1992. In: *Ecosystem Modeling as a Management Tool for the Black Sea*, L. Ivanov and T. Oguz (eds). NATO ASI Series, Environmental Security-Vol.47, Kluwer Academic Publishers, Vol. 2, pp. 69–92.
- Oguz, T., H. Ducklow, P. Malanotte-Rizzoli, J.W. Murray, V.I. Vedernikov, and U. Unluata, 1999. A physical-biochemical model of plankton productivity and nitrogen cycling in the Black Sea. *Deep-Sea Res. I*, **46**, 597–636.
- Oguz, T., H. W. Ducklow, and P. Malanotte-Rizzoli, 2000. Modeling distinct vertical biogeochemical structure of the Black Sea: Dynamical coupling of the Oxic, Suboxic and Anoxic layers. *Global Biogeochem. Cycles*, **14**, 1331–1352.
- Oguz, T., J. W. Murray, and A. E. Callahan, 2001a. Modeling redox cycling across the suboxic-anoxic interface zone in the Black Sea. *Deep-Sea Res. I*, **48**, 761–787.
- Oguz, T., H. W. Ducklow, J. E. Purcell, and P. Malanotte-Rizzoli, 2001b. Modeling the response of top-down control exerted by gelatinous carnivores on the Black Sea pelagic food web. *J. Geophys. Res.*, **106**, 4543–4564.
- Oguz, T., P. Malanotte-Rizzoli, and H.W. Ducklow, 2001c. Simulations of phytoplankton seasonal cycle with multi-level and multi-layer physical-ecosystem models: The Black Sea example. *Ecological Modelling*, **144**, 295–314.
- Oguz, T., A. G. Deshpande, and P. Malanotte-Rizzoli, 2002a. On the Role of Mesoscale Processes Controlling Biological Variability in the Black Sea: Inferences From SeaWIFS-derived Surface Chlorophyll Field. *Continental Shelf Research*, **22**, 1477–1492.
- Oguz, T., P. Malanotte-Rizzoli, H.W. Ducklow, J.W. Murray, 2002b. Interdisciplinary studies integrating the Black Sea biogeochemistry and circulation dynamics. *Oceanography*, **15(3)**, 4–11.

- Oguz, T., T. Cokacar, P. Malanotte-Rizzoli, and H. W. Ducklow, 2003. Climatic warming and accompanying changes in the ecological regime of the Black Sea during 1990s. *Global Biogeochem. Cycles*, **17**(3), 1088, doi:10.1029/2003.
- Ozsoy, E. and U. Unluata, 1997. Oceanography of the Black Sea: a review of some recent results. *Earth Sci.Rev.*, **42**, 231–272.
- Ozsoy, E., U. Unluata and Z. Top, 1993. The Mediterranean water evolution, material transport by double diffusive intrusions and interior mixing in the Black Sea. *Prog. Oceanogr.*, **31**, 275–320.
- Ozsoy, E., D. Di Iorio, M. C. Gregg, and J.O. Backhaus, 2001. Mixing in the Bosphorus Strait and the Black Sea continental shelf: observations and a model of dense water outflow. *J. Mar. Syst.*, **31**, 99–135.
- Ozsoy, E., D. Rank, and I. Salihoglu, 2002. Pycnocline and deep mixing in the Black Sea: stable isotope and transient tracer measurements. *Estuarine, Coastal and Shelf Science*, **54**, 621–629.
- Peneva, E., E. Stanev, V. Belokopytov, and P.Y. Le Traon, 2001. Water transport in the Bosphorus Strait estimated from hydro-meteorological and altimeter data: seasonal and decadal variability. *J. Mar. Syst.*, **31**, 21–33.
- Polat, S.Ç. and S., Tugrul, 1995. Nutrient and organic carbon exchanges between the Black and Marmara Seas through the Bosphorus Strait. *Continental Shelf Research*, **15**, 1115–1132.
- Porumb F., 1989. The influence of eutrophication on zooplankton communities in the Black Sea waters. *Certerari Marine*, **22**, 233.246.
- Rachev, N.H., E.V. Stanev, 1997. Eddy processes in semi-enclosed seas. A case study for the Black Sea. *J. Phys. Oceanogr.*, **27**, 1581–1601.
- Rass, T.S., 1992. Changes in the fish resources of the Black Sea. *Oceanology (Eng. Trans.)*, **32**, 197–153.
- Repeta, D.J. and D.J. Simpson, 1991. The distribution and recycling of chlorophyll, bacteriochlorophyll and carotenoids in the Black Sea. *Deep-Sea Res.*, **38**, Suppl.2A, S969-S984.
- Repeta, D.J., D.J. Simpson, B.B Jorgensen, and H.W. Jannash, 1989. Evidence for anoxic photosynthesis from distribution of bacteriochlorophylls in the Black Sea. *Nature*, **342**, 69–72.
- Ross D.A. and E.T. Degens, 1974. Recent sediments of the Black Sea. In: *The Black Sea-Geology, Chemistry, and Biology*, Degens.E.T and Ross.D.A, eds, American Association of Petroleum Geologists Memoir Vol.20, Tulsa, Oklahoma, U.S.A., pp. 183–199.
- Roazanov, A.G. 1996. Redox stratification in Black Sea waters. *Oceanology (Engl. Transl.)*, **35**, 500–504.
- Roazanov, A.G., L.N. Neretin, and I.I. Volkov, 1998. Redox Nepheloid Layer (RNL) of the Black Sea: Its location, composition and origin. In: *Ecosystem Modeling as a Management Tool for the Black Sea*. L. Ivanov and T. Oguz, eds. NATO ASI Series, 2-Environmental Security-47, Kluwer Academic Publishers, Vol. 1, pp. 77–92.
- Ryan, W.B.F. and W.C. Pitman, 1999. Noah's Flood: The new scientific discoveries about the event that changed history. Simon and Schuster, New York, 319p.
- Ryan, W.B.F., W.C. Pitman, C.O. Major, K. Shimkus, V. Moskalenko, G.A. Jones, P. Dimitrov, N. Gorur, M. Sakinc, and H. Yuçe, 1997: An abrupt drowning of the Black Sea shelf. *Marine Geology*, **138**, 119–126.
- Ryan, W.B.F., C.O. Major, G. Lericolais, S.L. Goldstein, 2003. Catastrophic flooding of the Black Sea. *Annu. Rev. Earth Planet. Sci.* **31**, 525–554.
- Saydam, C., S. Tugrul, O. Basturk, and T. Oguz, 1993: Identification of the oxic/anoxic interface by isopycnal surfaces in the Black Sea. *Deep Sea Research*, **40**, 1405–1412.
- Shaffer, G., 1986: Phosphate pumps and shuttles in the Black Sea. *Nature*, **321**, 515–517.
- Shiganova, T.A., 1998: Invasion of the Black Sea by the ctenophore *Mnemiopsis leidyi* and recent changes in pelagic community structure, *Fish. Oceanogr.*, **7**, 305–310.
- Shiganova, T.A., Yu. V. Bulgakova, S.P. Volovik, Z.A. Mirzoyan, and S.I. Dudkin, 2001: The new invader *Beroe ovata* Mayer 1912 and its effect on the ecosystem in the northeastern Black Sea. *Hydrobiologia*, **451**, 187–197.

- Shushkina, E.A., M.E. Vinogradov, L.P. Lebedeva, T. Oguz, N.P. Nezlin, V. Yu. Dyakonov, and L.L. Anokhina, 1998: Studies of structural parameters of planktonic communities of the open part of the Black Sea relevant to ecosystem modeling. In: *Ecosystem Modeling as a Management Tool for the Black Sea*, vol. 1, NATO Sci. Partnership Sub-ser., 2, vol. 47, L.I. Ivanov, and T. Oguz, eds. Kluwer Acad., Norwell, Mass., pp. 311–326.
- Simo, R., 2001. Production of atmospheric sulfur by oceanic phytoplankton: biogeochemical, ecological and evolutionary links, *TRENDS in Ecology & Evolution*, **16**, 287–294.
- Sokolova, E., E.V. Stanev, V. Yakubenko, I. Ovchinnikov, R. Kosyan, 2001. Synoptic variability in the Black Sea. Analysis of hydrographic survey and altimeter data. *J. Mar. Syst.*, **31**, 45–63.
- Sorokin, Y.I., 1972. The bacterial population and the process of hydrogen sulfide oxidation in the Black Sea. *J. Conseil Int. pour l'Exploration de la Mer*, **34**, 423–454.
- Sorokin, Y.I., 2002. *The Black Sea ecology and oceanography*. Backhuys Publishers, Leiden, 875 pp.
- Spencer, D.W. and P.G. Brewer, 1971. Vertical advection, diffusion and redox potentials as controls on the distribution of manganese and other trace metals dissolved in waters of the Black Sea. *J. Geophys. Res.*, **76**, 5877–5892.
- Stanev, E.V., 1990. On the mechanisms of the Black sea circulation. *Earth-Sci. Rev.*, **28**, 285–319.
- Stanev, E. V. and J.M. Beckers, 1999. Numerical simulations of seasonal and interannual variability of the Black Sea thermohaline circulation. *J. Mar. Syst.*, **22**, 241–267.
- Stanev, E. V. and N.H. Rachev, 1999. Numerical study of the planetary Rossby modes in the Black Sea. *J. Mar. Syst.*, **21**, 283–306.
- Stanev, E.V., J.V. Staneva and V.M. Roussenov, 1997. On the Black Sea water mass formation. Model sensitivity study to atmospheric forcing and parameterization of some physical processes. *J. Mar. Syst.*, **13**, 245–272.
- Stanev, E.V. and J.V. Staneva, 2000. The impact of the baroclinic eddies and basin oscillations on the transition s between different quasi-stable states of the Black Sea circulation. *J. Mar. Syst.*, **24**, 3–26.
- Stanev, E.V. and E. Peneva, 2002. Regional sea level response to global climatic change: Black Sea examples. *Global and Planetary Changes*, **32**, 33.47.
- Staneva, J.V. and E.V. Stanev, 2002. Water mass formation in the Black Sea during 1991–1995. *J. Mar. Syst.*, **32**, 199–218.
- Staneva, J.V., K.O. Buesseler, E.V. Stanev, and H.D. Livingston, 1999. The application of radiotracers to a study of Black Sea circulation: validation of numerical simulations against observed weapons testing and Chernobyl ¹³⁷Cs data. *J. Geophys. Res.*, **104**, 11099–11114.
- Staneva, J.V., D.E., Dietrich, E.V., Stanev, M.J., Bowman, 2001. Rim Current and coastal eddy mechanisms in an eddy-resolving Black Sea general circulation model. *J. Mar. Systems*, **31**, 137–157.
- Stanley, D.J., and C. Blanpeid, 1999. Late Quaternary water exchange between the eastern Mediterranean and the Black Sea. *Nature*, **285**, 537–541.
- Sur, H.I. and Y.P. Ilyin, 1997. Evolution of satellite derived mesoscale thermal patterns in the Black Sea. *Prog. Oceanogr.*, **39**, 109–151.
- Sur, H.I., E., Ozsoy, U., Unluata, 1994. Boundary current instabilities, upwelling, shelf mixing and eutrophication processes in the Black Sea. *Prog. Oceanogr.*, **33**, 249–302.
- Sur, H.I., E., Ozsoy, Y.P., Ilyin, U., Unluata, 1996. Coastal/deep ocean interactions in the Black Sea and their ecological/environmental impacts. *J. Marine Systems*, **7**, 293–320, 1996.
- Tebo, B.M., 1991. Manganese(II) oxidation in the suboxic zone of the Black Sea. *Deep-Sea Res.*, **38**, Suppl.2A, S883-S906.
- Tebo, B.M., R.A. Rosson, and K.H. Neelson, 1991. Potential for manganese (II) oxidation and manganese (IV) reduction to co-occur in the suboxic zone of the Black Sea. In: *Black Sea Oceanography*, E.Izdar and J.W. Murray, eds. NATO ASI Series C-Vol.351, Kluwer Academic Publishers, pp. 173–186.

- Titov, V.B., 2000. Dependence of the formation of the winter hydrological structure in the Black Sea on the severity of winter conditions. *Oceanology (Engl. Transl.)*, **40**, 777–783.
- Tugrul, S. 1993. Comparison of TOC concentrations by persulphate-UV and HTCO techniques in the Marmara and Black Seas. *Marine Chemistry*, **41**, 265–270.
- Tugrul, S., O. Basturk, C. Saydam, and A. Yilmaz, 1992. The use of water density values as a label of chemical depth in the Black Sea. *Nature*, **359**, 137–139.
- Unluata, U., T. Oguz, M.A. Latif and E. Ozsoy, 1989. On the physical oceanography of Turkish straits. In: *The physical oceanography of sea straits*, L.J. Pratt, eds. NATO ASI Series, Kluwer, The Netherlands.
- Uysal, Z., A. E. Kideys, L. Senichkina, L. Georgieva, D. Altukhov, L. Kuzmenko, L. Manjos, and E. Eker, 1998. Phytoplankton patches formed along the southern Black Sea coast in spring and summer 1996. In: *Ecosystem Modeling as a Management Tool for the Black Sea*, L. I. Ivanov and T. Oguz, eds. vol 1, Kluwer Academic Publishers, Netherlands, pp. 151–162.
- Vedernikov, V.I. and A.B. Demidov, 1997. Vertical distributions of primary production and chlorophyll during different seasons in deep part of the Black Sea, *Oceanology, (English trans.)*, **37**, 376–384.
- Vinogradov, M.E., and Yu.R. Nalbandov, 1990. Effect of changes in water density on the profiles of physicochemical and biological characteristics in the pelagic ecosystem of the Black Sea. *Oceanology (English trans.)*, **30**, 567–573.
- Vinogradov, M.E., E.A. Shushkina, L.L. Anokhina, S.V. Vostokov, N.V. Kucheruk, and T.A. Lukashova, 2000. Mass development of the ctenophore *Beroe ovata* Eschscholtz near the northeastern coast of the Black Sea. *Oceanology (Engl. Transl.)*, **40**, 52–55.
- Yakushev, E.V., 1998. Mathematical modeling modeling of oxygen, nitrogen, sulfur and manganese cycling in the Black Sea. In: *Ecosystem Modeling as a Management Tool for the Black Sea*, L. Ivanov and T. Oguz, eds. NATO ASI Series, 2-Environmental Security-47, Kluwer Academic Publishers, Vol. 2, pp. 373–384.
- Yakushev, E.V. and L.N. Neretin, 1997. One dimensional modeling of nitrogen and sulfur cycles in the aphotic zone of the Black and Arabian Seas. *J. Global Biogeochemical Cycles*, **11**, 401–414.
- Yakushev, E.V., D.E. Besedin, Yu. F. Lukashev, and V.K. Chasovnikov, 2001. On the rise of the upper boundary of the anoxic zone in the density field of the Black Sea. *Oceanology (Eng. Transl.)*, **41**, 654–659.
- Yanko, V., J. Kennett, H. Koral, J. Kronfield, 1999. Stable isotope evidence from the Holocene Sea of Marmara sediments for two-way watermass interchange between the Black Sea and the Mediterranean Sea. *S. Afr. J. Sci.*, **95**, 201–204.
- Yilmaz, A., S. Tugrul, C. Polat, D. Ediger, Y. Coban, and E. Morkoc, 1998a. On the production, elemental composition (C,N,P) and distribution of photosynthetic organic matter in the Southern Black Sea. *Hydrobiologia*, **363**, 141–156.
- Yilmaz, A., O.A. Yunev, V.I. Vedernikov, S. Moncheva, A.S. Bologa, A. Cociasu, and D. Ediger, 1998b. Unusual temporal variations in the spatial distribution of chlorophyll-a in the Black Sea during 1990–1996. In: *Ecosystem Modeling as a Management Tool for the Black Sea*. L. Ivanov and T. Oguz, eds., NATO ASI Series, 2, Environment-Vol.47, Kluwer Academic Publishers, Vol. 1, pp. 105–120.
- Yunev, O.A., V.I. Vedernikov, O. Basturk, A. Yilmaz, A. E. Kideys, S. Moncheva, and S. Kononov, 2002. Long-term variations of surface chlorophyll-a and primary production in the open Black Sea, *Mar. Ecol. Prog. Ser.*, **230**, 11–28.
- Zaitsev, Yu. and V. Mamaev, 1997. *Marine Biological Diversity in the Black Sea: A Study of Change and Decline*, GEF Black Sea Environmental Programme, United Nations Publications, 208pp.
- Zatsepin, A.G., A.I. Ginzburg, A.G. Kostianoy, V.V. Kremenitskiy, V.G. Krivosheya, S.V. Stanichny, P-M. Poulain, 2003. Observations of Black Sea mesoscale eddies and associated horizontal mixing. *J. Geophys. Res.*, **108**, 3246, doi:10.19/2002JC001390.

